Universidade de Lisboa

Faculdade de Farmácia

Development of pH-sensitive Polymeric Nanoparticles for Targeted Drug Delivery to the Ischemic Heart

Gonçalo Alexandre da Conceição Duarte Marques

Mestrado Integrado em Ciências Farmacêuticas

2017

Universidade de Lisboa

Faculdade de Farmácia

Development of pH-sensitive Polymeric Nanoparticles for Targeted Drug Delivery to the Ischemic Heart

Gonçalo Alexandre da Conceição Duarte Marques

Monografia de Mestrado Integrado em Ciências Farmacêuticas

apresentada à Universidade de Lisboa através da Faculdade de Farmácia

Orientador: Prof. Doutor João Fernandes de Abreu Pinto

Co-Orientador: Prof. Doutor Hélder Almeida Santos

2017

ABSTRACT

Heart failure post-myocardial infarction remains one of the global leading causes of mortality. The therapeutics, available today, only ameliorate the symptoms, without having any preventive effect on the, functional and structural, heart-remodeling process that ensues after such ischemic event. For this, lately, nanotechnology has emerged as a possible alternative to overcome countless limitations of conventional cardiovascular medicine. The present study focus on the preparation of nanoparticles with resort to the emulsification and solvent evaporation method, using the spermine-modified acetalated dextran as polymer for selective drug delivery of a cardioprotective drug. Additionally, it dwells on the subsequent functionalization resorting to crosslinking chemistry and using propylene glycol as a bioconjugate, given its hydrophilic properties and ability to prolong the nanoparticles' plasma half-life. The process and formulation variables, explored in this investigation, whether on preparation or functionalization, revealed to be of crucial importance to the nanosystem's characteristics. The optimization, on propylene glycol conjugation, was not possible, for the drug-loaded nanoparticles, within the time frame set for the experimental work. Upon PEGylation, major improvements were verified in colloidal stability (assessed in cell culture medium) and cytocompatibility (assessed in rat myoblasts). The drug release did not follow the pH-sensitive solubility pattern of the polymer, that is, with burst release in acidic conditions and sustained release in neutral pH. Several points to take in consideration and suggestions, for future work, are presented on how to refine this platform for intracellular nanodelivery.

Keywords: Heart Failure; Myocardial Infarction; Nanoparticles; Spermine-modified acetalated dextran; Pegylation

RESUMO

Uma das principais causas de mortalidade, a nível global, continua a ser insuficiência cardíaca pós-enfarte do miocárdio. As terapêuticas atualmente disponíveis apenas atenuam os sintomas, sem qualquer efeito de prevenção no processo de remodelação cardíaca, funcional e estrutural, que se inicia após o episódio de isquemia. Por isto, a nanotecnologia tem, ultimamente, emergido como uma possível alternativa para superar as inúmeras limitações da terapia cardiovascular convencional. O presente estudo foca-se na preparação de nanopartículas recorrendo ao método de emulsificação e evaporação do solvente, utilizando como polímero dextrano modificado com grupos acetais e espermina para a veiculação seletiva de um fármaco cardio-protetor. Adicionalmente, incide na posterior funcionalização recorrendo a química de reticulação e utilizando como biconjugado o propilenoglicol, atendendo às suas propriedades hidrofílicas e capacidade de prolongar a semivida das nanopartículas no plasma. As variáveis de processo e formulação, exploradas nesta investigação, quer na preparação quer na funcionalização, revelaram ter uma importância crucial nas características do nano-sistema. A otimização da conjugação com propilenoglicol não foi possível para as nanopartículas com fármaco, dentro da janela temporal concebida para o trabalho experimental. Após a peguilação, foram verificadas claras melhorias na estabilidade coloidal (avaliada em meio de cultura) e citocompatibilidade (avaliada em mioblastos de rato). A libertação do fármaco não seguiu o padrão da solubilidade do polímero, sensível ao pH, isto é, com libertação imediata em condições ácidas e libertação retardada a pH neutro. Diversas considerações a ter em conta e sugestões, para futuros trabalhos, são apresentadas no sentido de aperfeiçoar esta plataforma de nano-veiculação intracelular.

ACKNOWLEDGEMENTS

The laboratory work in this study was carried out at the Division of Pharmaceutical Technology, Faculty of Pharmacy, University of Helsinki during the Erasmus Plus Program, for the months of February to April, in the year of 2017.

First and foremost, I would like to express my deepest gratitude to my three supervisors: Professor João Pinto, Professor Hélder Santos and Mónica Ferreira (MSc.) for their patient guidance and enthusiastic encouragement. What is more, their invaluable scientific input and mentoring advice impacted this study in such a way that it would otherwise not exist at all.

I am also extremely grateful to my parents, my brother and my godmother for this accomplishment is yours as much as it is mine. Five years ago, all of them embarked with me on this journey, as a bedrock of unwavering belief and everlasting support.

Finally, I would like to dedicate this achievement to all my friends and colleagues, the ones whom I met throughout the Pharmacy degree, the Erasmus ones who made a place "cold and dark" feel like home and the ones that came before and shall come in the future. I have in them my source of fierce motivation and joyful inspiration.

To all the above, I cannot, by all means, thank you enough.

ABBREVIATIONS

AB	*Acetate Buffer*
AcDex	*Acetalated Dextran*
AcDexSp	*Spermine-modified AcDex*
AcDexSp-PEG	*PEG-functionalized-AcDexSp Nanocomposite*
ATR	*Attenuated Total Reflectance*
C1	*3,4,5-trisubstituted Isoxazole*
C1@AcDexSp	*C1 encapsulated AcDexSp Nanocomposite*
C1@AcDexSp-PEG	*C1 encapsulated PEG-functionalized-AcDexSp Nanocomposite*
CCM	*Cell Culture Medium*
CP	*Cardioprotective*
CV	*Cellular Viability*
DCM	*Dichloromethane*
DLS	*Dynamic Light Scattering*
DMEM	*Dulbecco's Modified Eagle Medium*
EDC	*1-Ethyl-3-(3-dimethylaminopropyl)-carbodiimide*
EE	*Encapsulation Efficiency*
ELS	*Electrophoretic Light Scattering*
EtOH	*Ethanol*
FBS	*Fetal Bovine Serum*
FTIR	*Fourier-transform Infrared Spectroscopy*
HBSS	*Hank's Balanced Salt Solution*
HEPES	*4-(2-hydroxyethyl)-1-piperazineethanesulfonic Acid*
HF	*Heart Failure*
HPLC	*High-performance Liquid Chromatography*
MeOH	*Methanol*
MES	*2-(N-morpholino)ethanesulfonic Acid*
MI	*Myocardial Infarction*
NHS	*N-hydroxysuccinimide*
NP	*Nanoparticles*
PBS	*Phosphate Buffer Saline*
PDI	*Polydispersity Index*
PEG	*Polyethylene Glycol*
PVA	*Polyvinyl Alcohol*
Sulfo-NHS	*N-hydroxysulfoxuccinimide*
TEA	*Triethanoloamine*
TEM	*Transmission Electron Microscopy*
ZP	*Zeta Potential*

TABLE OF CONTENTS

LIST OF FIGURES

LIST OF TABLES

1. INTRODUCTION

1.1. NANOTECHNOLOGY IN CARDIOVASCULAR DISEASE

Atherosclerotic cardiovascular diseases continue to be one of the leading causes of death worldwide, with the majority of mortality resulting from heart failure (HF) post-myocardial infarction (MI) and half of those diagnosed with severe HF dying within five years (1–5).

The first stage of atherosclerotic plaque formation is the activation of endothelial cells of artery walls, due to genetic disorders or numerous environmental risk factors (6). Monocytes' migration occurs, accompanied by the maturation and assembly of the former into macrophages and the latter towards foam cells (7). The smooth muscle cells proliferation, along with the progressive synthesis of extracellular matrix, provide fertile ground for lipids, cholesterol crystals and micro-vessels to create a necrotic central core, which substantially increases the risk of plaque rupture and MI (8).

A severe ischemic event, as in reduce blood supply to the heart with consequential shortage of oxygen, results in MI, an incident characterized by a massive loss of cardiomyocytes, which cannot be replenished by the adult human heart due to the limited innate proliferative capacity of these cells (9–12). Afterwards, a succession of complex and irreversible responses lead to adjustments in the cardiac muscle structure and/or function, where the degree of injury depends on the location and time following the event (11–13). The affected myocardial region is replaced by fibrotic scar tissue, which ensues progressive contractile dysfunction and pathological remodeling of the left ventricular wall, both which, in turn, ultimately lead to HF (11,14).

In clinical practice, revascularization strategies, followed by palliative care, are the standard care for acute MI (15,16). However, these approaches only ameliorate symptoms without treating the injury at the source and there is no therapy for the heart-remodeling process that arises post-MI. On a similar note, the only options for patients with end-stage HF are either heart transplantation, for which few donors are available, or left-ventricular assist devices, which increase the risk of stroke (17).

While extensive efforts have been made do prevent, limit or event treat MI and HF, there is still no up to date answer on how to successfully restore the function of an injured heart. Considering the urgency to restrain mortality, morbidity, healthcare costs and the rising prevalence of such diseases, one must highlight the impeding need for innovative solutions and the prospect of nanotechnology to come in handy (18,19).

Nanotechnology has had a tremendous impact in the research field. Among many novel nanomedicine approaches, some have been envisioned, applied and developed as nanosized vectors for delivery of therapeutics to the ischemic heart, given their unique abilities in

overcoming countless limitations of conventional cardiovascular medicine (11,12,20–29). One of nanoparticles' (NP) major advantages lies with the possibility of intravenous administration (30). This is particularly important in clinical practice, if one considers that the administration of potential cardioprotective (CP) new alternatives is often performed locally, with such drawbacks as the procedure requiring highly trained personnel and being invasive, costly and prone to complications (31).

1.2. SINGLE EMULSION AND SOLVENT EVAPORATION METHOD

Solvent evaporation method remains the most useful method for drug encapsulation, despite the numerous others techniques that have been reported (32,33). The drug encapsulation by solvent evaporation is widely applied in pharmaceutical industry to attain controlled release, mainly because these fabricated nanospheres have outstanding benefits such as: reducing the dose frequency, increasing patient's compliance and drug targeting to specific locations, all of which result in an overall higher clinical efficiency (34,35).

The choice among the different solvent evaporation methods depends on the hydrophilicity or hydrophobicity of the drug, being as for moderately water soluble or water soluble compounds a poor entrapment of the drug will ensue unless one resorts to a double emulsion (32,36).

For insoluble or poorly water-soluble drugs, the oil-in-water method (represented in Fig. 1) is usually employed. First, the polymer is dissolved or dispersed in an organic solvent, followed by dissolution of the hydrophobic drug in the organic solvent containing the polymer. Next, the organic phase is emulsified, through high shear homogenization or sonication, in an aqueous solution, using a surfactant (concept which is clarified bellow), to form a stable oil-in-water emulsion. Finally, the organic phase is allowed to evaporate with the formation of a suspension of NP, which may then be recovered by centrifugation, filtration or lyophilization (36,37).

Surfactants are amphiphilic molecules, which means that one part of the molecule is hydrophilic - has more affinity towards polar solutes such as water - and the other one is hydrophobic - has more affinity towards non-polar solutes such as hydrocarbons. These, also named, tensioactive agents, are consistently applied in the dispersion of one phase in another immiscible one, governing the effectiveness of the emulsion formation. These molecules tend to align themselves at the surface of the droplets reducing the surface tension, that is, lowering the free energy at the interface between the two phases (oil and water) and thus stabilizing the obtained emulsion - by avoiding the agglomeration and coalescence of the droplets during the emulsification process (36–38).

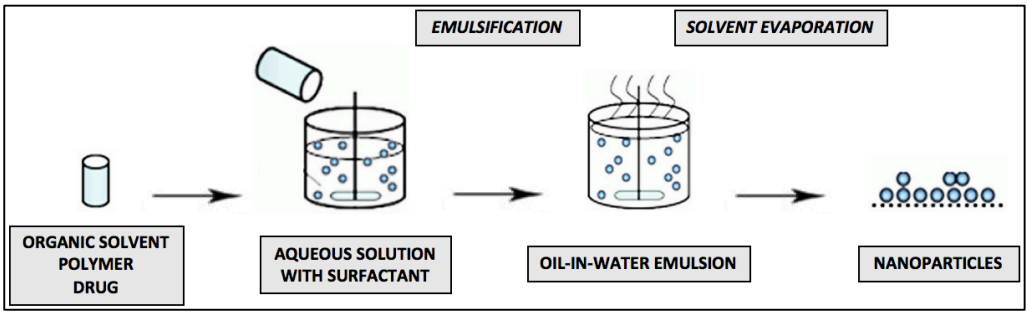

Fig. 1 - Basic steps for the single emulsion and solvent evaporation technique

1.3. SPERMINE-MODIFIED ACETALATED DEXTRAN

Polymers whose shape and/or solubility is modified in response to a stimulus have many biomedical applications in which targeted drug delivery is desired (39). One of the most prominent avenues for controlled release has to do with the exploitation of *in vivo* natural pH differences by using pH-sensitive polymers (40). These polymers are relatively stable at the extracellular pH of 7.4 yet quickly degrade, and thus selectively release the payload, under mildly acidic conditions as those which may be found in sites of inflammation, lysosomal compartments or in tumor tissue (41–43) This localized discharged of the therapeutic agent allows for dose-sparing with increased efficacy and reduced toxic side effects (44,45).

Dextran, a bacterially derived homopolysaccharide of glucose, has a history of human use in clinical applications for plasma volume expansion and substitution (46). Therefore, it appeared to be well poised for a solubility switching mechanism envision, so that its solubility in water or organic solvents could be reversibly modified. In fact, it can be rendered insoluble in water in the form of acetalated dextran (AcDex), by turning dextran's hydroxyl groups into acetal-protecting groups. In contrast, in acidic environments, AcDex undergoes degradation with the pendant acetal groups hydrolysis unmasking the parent hydroxyl groups and so the organic-soluble AcDex is converted back into the water-soluble dextran, as depicted in Fig. 2 (42,47).

AcDex is considered to be biodegradable due to its innocuous byproducts: dextran (a sugar), acetone (a nontoxic and common metabolite intermediate) and methanol (MeOH) (nontoxic in small quantities) for acyclic acetals and dextran and acetone only for the cyclic ones (42,48,49). Furthermore, it figures among the most promising pH-sensitive biopolymers for the reasons stated ahead. Firstly, its uniqueness in the sense that, unlike the other commonly used polymers, its decomposition products are of neutral pH hence ensuring that the encapsulated cargos are not harmed. Secondly, its degradation rate being easily tunable through the acetal coverage, which is, in turn, governed by the synthesis reaction time - a longer reaction time entails a high degree of thermodynamically stable cyclic acetals (marked

in light blue, Fig. 2) which take time to hydrolyze, whereas shorter reaction times produce more kinetically favored acyclic acetals (marked in dark blue, Fig. 2) which hydrolyze quickly (49,50). And finally its facile synthesis which is, in a nutshell, a single vessel reaction with subsequent purification through precipitation (51).

The acetalated-polymer has been extensively studied and revealed to be particularly promising for the development of biocompatible delivery platforms (52–55). This does not come as a surprise if ones takes into consideration that its termini can be easily functionalized (56,57). For example, through reductive amination chemistry it is possible to form spermine-modified AcDex (AcDexSp), which besides inheriting the pH-responsiveness of AcDex introduces new features such as enhancement of cellular uptake (since the polymer becomes cationic) and the ability for further conjugation (since the termini amine groups are more reactive) (43,54,55).

AcDex microparticles have been reported in terms of potential as a delivery vehicle for therapeutics to the heart post-MI. Suarez *et al.* achieved tunable release, between days and weeks, unlike other materials previously tested which have define release rates in the ischemic environment. For this, it was only required to vary the reaction time so that the ratio of cyclic and acyclic acetals could be adjustable. They also took advantage of the polymer's pH-sensitivity since mildly acidic conditions may be found in ischemic tissue (pH 6.0-7.0) (17). Later on, Suarez *et al.* demonstrated optimal timing for delivery of CP molecules, as releasing of multiple factors over a wide range of time frames enabled positive tissue remodeling following ischemic damage post-MI (58).

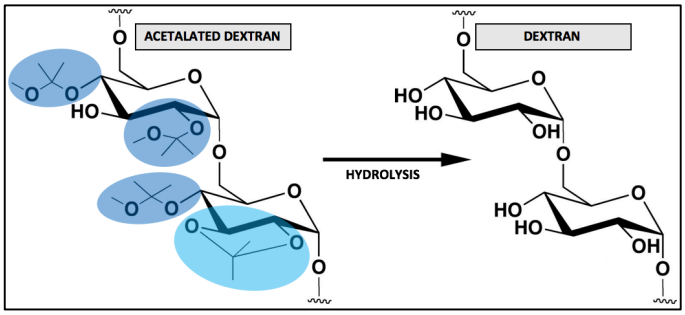

Fig. 2 - AcDex and dextran chemical structures

1.4. BIOCONJUGATION

Bioconjugation entails the chemical interaction of biologically active molecules, the so-called functional groups, to NP, which via upgrading their stability, functionality and biocompatibility render them ideal for clinical applications (59).

Among these functional groups, polyethylene glycol (PEG) is the most widely employed to prolong nanocarriers plasma half-life since. In *in vivo* applications, the opsonins (portions of

the plasma proteins which adsorb to the surface) may endorse non PEG-modified NP recognition by the mononuclear phagocyte system and consequently lead to their rapid removal from the bloodstream (60–63). Seeing as phagocytic cells are negatively charged, depending on the NP' surface, these opsonins can be crucial to avoid repulsion and endorse engulfment and transport of the material for degradation (in the liver and the spleen) and excretion (in the kidneys) (64,65).

In other words, PEGylated NP have the ability to evade uptake by the reticuloendothelial system and are able to remain in the systemic circulation with an enhanced permeability and retention effect verified in the diseased-affected area (64,66). Besides, PEG is responsible for the so-called "stealth" behavior for diminishing the NP interaction with non-targeted molecules. Moreover, due to its hydrophilic ethylene glycol repeats, solubility in serum is increased. For all of this, PEG establishes itself as the gold-standard cloaking agent (64,67,68).

Sun *et al.* demonstrated PEGylation's ability to prolong *in vivo* NP' half-life and hence significantly enhance longevity of its therapeutic action, since PEGylated NP, administered at much lower frequency than their unmodified parental molecules, produce similar extent of benefit and displayed comparable binding affinity to glucagon-like peptide-1 receptors. In short, PEGylated NP, functionalized with exendin-4, showed a CP effect in heart failure induced by MI (69).

Zhang *et al.* determined that PEGylated lipid-based NP loaded with baicalin, which has been proved to ameliorate acute MI, improved the pharmacokinetics profile with a prolonged circulation time and thus an increase in the area under the curve. Furthermore, PEG was shown to enable decrease of infarct size on the heart due to passive targeted delivery to the ischemic area with greater local NP' concentration (70).

Shao et al. confirmed that the PEGylation of heart-targeted NP could improve their plasma half-life and also provide a sustained and persistent release of loaded CP drugs (71).

1-Ethyl-3-(3-dimethylaminopropyl)-carbodiimide (EDC)-N-hydroxysuccinimide (NHS)-mediated reaction is one of the most attractive approaches and has been extensively applied in the conjugation of biomolecules onto different substrates due to its high conversion efficiency, mild reaction conditions and excellent biocompatibility with little to no effect on the bioactivity of the target molecules (72).

Through EDC/NHS (zero-length crosslinking agents) coupling chemistry, the terminal carboxylic groups (of the PEG molecules) can be reacted with primary amines (of the AcDexSp NP' surface) to yield an amide bond (73). This mechanism is represented in Fig 3. and thoroughly explained below.

EDC, a water-soluble carbodiimide, reacts with the carboxylic moiety to form an O-acylisourea intermediate that is prone to degradation. The latter might take place as hydrolysis

(to regenerate acid groups), dehydration (with neighboring carboxylic acids to produce an anhydride) or intramolecular acyl rearrangement (to form N-acylurea). In spite of this, this O-acylisourea reactive ester, when in contact with N-hydroxysulfoxuccinimide (Sulfo-NHS) (the water-soluble analog of NHS), is stabilized by means of conversion to an amine-reactive semi-stable Sulfo-NHS ester (74–77). At last, upon exposure of such active ester to primary amines, a nucleophilic attack takes place and a covalent bond is formed between the PEG molecule and the surface of the NP (78,79).

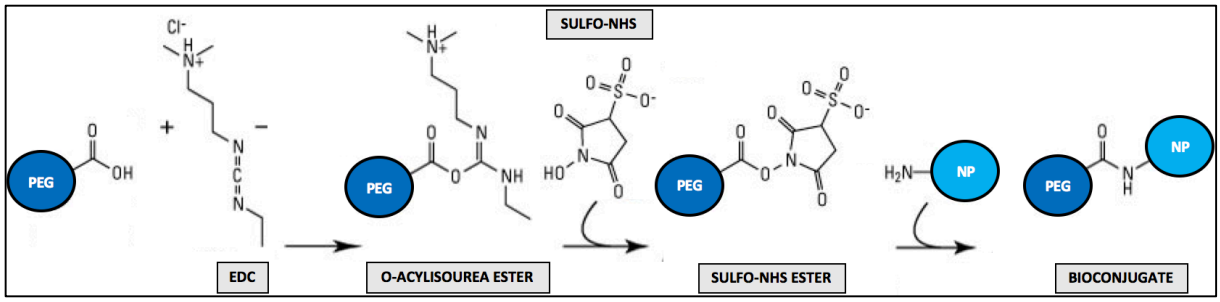

Fig. 3 - Mechanism of bioconjugation through EDC/NHS coupling chemistry

1.5. KINETIC MODELING ON DRUG RELEASE

Drug release refers to the process in which drug solutes migrate from the inner polymeric matrix to the polymer's outer surface and, from there, to the release medium (80).

In general, the drug release rate from polymeric nanoparticle-based delivery systems depends on: drug solubility, desorption of the surface-bound or adsorbed drug, drug diffusion through the polymeric matrix, erosion of the NP' matrix (due to polymer degradation) and the combination of erosion and diffusion processes (81). Additionally, several other factors such as the drug-polymer interaction, the pKa of the drug and the amount of drug loaded in the NP can influence the drug release from nanostructured systems (82).

Taking into account that mathematical models development requires in-depth knowledge of the ensemble of phenomena ruling release kinetics, they turn out to have a great value in the process of formulation optimization, mostly because an accurate prediction of the drug release profile will lead the way to better therapeutic efficacy and safety use of such drug (83–85).

Nevertheless, a mathematical model is focused on one or two dominant release-driving forces, so it comes as no surprise that some disconnections may be found between literature and experimental data, since there are multiple complex driving forces in a single release process (80). Therefore, mathematical modeling may, indeed, be merely perceived as a "mathematical metaphor of some aspects of reality" (86).

A kinetic model is based on a mathematical function that describes the dissolution profile and elucidates about the solute transport mechanism (80,86). In order to find the ideal

one, one must proceed to the linear regression analysis of their corresponding functions (Table 1) (87). These kinetic model approach includes zero-order, first-order, Higuchi, Hixson-Crowell and Korsmeyer-Peppas, whose features are detailed in the Tables below. The first four are employed to determine the drug kinetics release, whereas Korsmeyer-Pepppas is a more generic equation whose exponent analysis describes the mechanism of drug release (Table 3) (82,86).

Table 1 - Functions of the various kinetic models (82,86–89)

	Equation	Parameters definition	Graphical plots
Zero-order	$C = k_0 \times t$	C: concentration of the drug k_0: zero-order rate constant t: time	Cumulative % drug released *vs.* time
First-order	$\log C_0 - \log C_t = k_1 t / 2.303$	C_0: initial concentration C_t: concentration at time t k_1: first-order rate constant t: time	Log cumulative % drug remaining *vs.* time
Higuchi	$Q = k_h \times t^{1/2}$	Q: amount of drug released at time t k_h: Higuchi constant t: time	Cumulative % drug released *vs.* square root of time
Hixson-Crowell	$Q_0^{1/3} - Q_t^{1/3} = k_{hc} \times t$	Q_0: initial amount of drug Q_t: remaining amount of drug at time t k_{hc}: Hixson-Crowell constant t: time	Cube root % drug remaining *vs.* time
Korsmeyer-Peppas	$M_t - M_\alpha = K_{kp} \times t^n$	$M_t - M_\alpha$: drug fraction release at time t k_{kp}: Korsmeyer-Peppas constant t: time n: release exponent	Log cumulative % drug released *vs.* log time *(Limited at the first 60% of cumulative release)*

Table 2 - Summarized characteristics of the various kinetic models (82,84,89–96)

	Release proportionality	Application in delivery systems	Release mechanism
Zero-order	Directly at time	- Transdermal systems - Osmotic systems - Insoluble matrices with low soluble drugs	Diffusion
First-order	At the amount of drug remaining	- Absorption and/or elimination of drugs - Porous matrices with water-soluble drugs	Diffusion
Higuchi	At the square root of time	- Transdermal systems - Insoluble matrices with water-soluble drugs	Diffusion
Hixson-Crowell	At the surface area of the system	- Various pharmaceutical forms such as tablets	Erosion

Table 3 - Korsmeyer-Peppas's interpretation of release mechanisms (82,86–88)

Release exponent (n)	Drug transport mechanism	Release mechanism
n < 0.5	Quasi-fickian diffusion	Partial diffusion
n = 0.5	Fickian diffusion *(identical to Higuchi model)*	Diffusion
0.5 < n < 1	Non-fickian (anomalous) transport	Diffusion and erosion
n = 1	Case II transport *(identical to zero-order model)*	Diffusion
n > 1	Super Case II transport	Erosion

2. AIMS OF THE STUDY

The specific objectives of the present work were as follows:

(1) To encapsulate a poorly water soluble drug into a pH-sensitive polymer by an oil/water single emulsion and solvent evaporation method, as well as optimize the NP preparation method in terms of organic solvent type, surfactant concentration, evaporation time, aqueous phase volume and polymer and drug amount;

(2) To functionalize, through EDC/NHS coupling chemistry, the surface of the NP with PEG for enhancement of their colloidal stability and cytocompatibility and optimize said conjugation reaction in terms of pH, ratio and time;

(3) To test the NP for cytocompatibility and colloidal stability, in a cardiac cell line and its cell culture medium (CCM), respectively;

(4) To verify a pH-driven degradation of the polymer matrix and subsequent drug release.

3. MATERIALS AND METHODS

3.1. NANOPARTICLES PREPARATION

The preparation of AcDexSp NP was based on an oil/water single emulsion and solvent evaporation method (41).

First, the AcDexSp polymer (12,5mg) was dissolved in dichloromethane (DCM) (0,25mL) and then the CP drug 3,4,5-trisubstituted isoxazole (C1) (1mg) (97) was added to this solution if drug-loaded NP were being prepared. Afterwards, an aqueous solution of polyvinyl alcohol (PVA) (Mw: 31000-50000g/mol, Sigma) (0,5mL, 2,5% w/v) was further added, followed by 30s of sonication on an ice bath, with an output setting of 5 and a duty cycle of 50%, using a probe sonicator (Vibra-cell VCX 750 ultrasonic processor, Sonics and Materials, Inc., USA). The emulsion formed was immediately poured into a second PVA aqueous solution (1.5mL, 0.2% w/v) and magnetically stirred at 300rpm for 3h to allow the evaporation of the organic solvent at room temperature. Next, the NP were recovered by centrifugation (16100g, 5min), re-suspended twice with 4-(2-hydroxyethyl)-1-piperazineethanesulfonic acid (HEPES) (pH 7.4, 10mM) and once with Milli-Q-water (pH 8.0), being that after each washing step the NP were pelleted while keeping all the supernatants for high-performance liquid chromatography (HPLC) detection.

Reverse phase HPLC (Agilent 1100 series HPLC system, Agilent Technologies, Germany) was used with Gemini® C_{18} column (Gemini-NX, 3mm C_{18}, 110 Å; Phenomenex, CA, USA) as the stationary phase and a mixture of phosphoric acid (0.1% v/v, pH 2.0) and MeOH (solvent ratios of 35:65 v/v) as the mobile phase. For detection, 20μl of standard drug solutions or sample solutions were injected. The flow rate was set at 0.9mL/min and determination at a wavelength of 280nm with a retention time of 4.489min. A standard plot of the drug, using MeOH as solvent, was generated over the concentration range of 0.25-128μg/mL and was found to be linear with r^2 value of 0,9941.

The encapsulation efficiency (EE) and loading degree (LD) were calculated by Eq. (1) and (2), respectively. Both of them were quantified by dissolving a known amount of NP in MeOH and then proceeding to HPLC analysis as previously described.

$$EE\ (\%) = \frac{Amount\ of\ drug\ in\ the\ NP\ (\mu g)}{Total\ amount\ of\ drug\ initially\ added\ (\mu g)} \times 100\ (1)$$

$$LD\ (\%) = \frac{Amount\ of\ drug\ in\ the\ NP\ (\mu g)}{Mass\ of\ the\ NP\ (\mu g)} \times 100\ (2)$$

In the previous emulsification-solvent evaporation process, the influence of several process and formulation variables (organic solvent type, surfactant concentration, polymer amount, evaporation time and aqueous phase volume and drug quantity) was studied on the preparation of AcDexSp drug-loaded NP. Each one of these variables was assessed at a time while keeping all the other variables and geometry of the fabrication system constant.

ORGANIC SOLVENT TYPE

Two solvents were tested with the AcDexSp polymer and the C1 drug: ethanol (EtOH) and DCM. The NP produced (n=4) with both solvents were characterized by dynamic light scattering (DLS), electrophoretic light scattering (ELS) and transmission electron microscopy (TEM).

SURFACTANT CONCENTRATION

In this investigation, a single non-ionic surfactant, PVA, was used in varying concentrations: 2 (n=1), 2.5 (n=2) and 3% (n=2) in order to find the optimal suitable condition for small and drug-loaded NP - with low size and polydispersity index (PDI) and high EE.

POLYMER AMOUNT, EVAPORATION TIME AND AQUEOUS PHASE VOLUME

Among these three parameters: polymer amount, evaporation time and aqueous phase volume (of the aqueous phase in the evaporation step) two possibilities were tested out: 12.5mg, 2h and 2.5mL (n=1) versus 25mg, 3h and 1.5mL (n=2).

DRUG QUANTITY

In order to further optimize NP' formulation, tryouts with two fractions of C1 drug: 1mg (n=3) and 4mg (n=5) were performed.

3.2. NANOPARTICLES FUNCTIONALIZATION

The surface of the NP was modified with PEG (CO2H-PEG-CO2H, Mw: 2000g/mol, Sigma-Aldrich, USA). A solution of EDC/NHS was prepared by adding 4μl of EDC and 1mg of NHS in proportion to 1ml of 2-(N-morpholino)ethanesulfonic acid (MES) buffer, while adjusting the pH to 7.0. First, PEG was dissolved in the previous solution followed by the NP in an optimized ratio of 1:10 (NP: PEG). The conjugation reaction ensued, magnetically stirred at 300rpm, for 4h and at room temperature. Finally, the PEGylated NP were pelleted by centrifugation (16100*g*, 5min) and washed twice with Milli-Q-water (pH 8.0).

Considering the vast amount of different NP and biomolecules reported so far, there are no standardized protocols for NP functionalization. Therefore, one must optimize the

bioconjugation conditions while aiming at providing a valid coupling strategy. In this PEGylation process, the influence of a few process and formulation variables (pH, NP:PEG ratio and reaction time and physical adsorption) was studied on the preparation of AcDexSp-PEG bare NP. Each one of these variables was assessed at a time while keeping all the other variables and geometry of the preparation method constant (98).

pH

The coupling was performed in MES buffer, which is a non-amine and non-carboxylate buffer and thus ensures no interference. Two protocols were examined: carboxyl activation at pH 5.0 with subsequent - before the addition of the NP - increase to 7.0 (n=1) versus entire coupling at pH 7.0 (n=1).

NP: PEG RATIO AND REACTION TIME

Two time points were tested against different NP: PEG ratios: 1:4, 2h (n=1); 1:4,4h (n=1); 1:2, 2h (n=1); 1:2, 4h (n=1); 2:1, 2h (n=1); 2:1, 4h (n=1); 4:1, 2h (n=1); 4:1, 4h (n=1).

PHYSICAL ADSORPTION

As a mean to certify the success of the functionalization, a physical mixture of PEG and NP (n=1) was compared to the optimized conjugation (n=3).

3.3. NANOPARTICLES CHARACTERIZATION

3.3.1. SIZE, PDI AND ZP

The size and PDI were performed using DLS with a Zetasizer Nano ZS (Malvern Instruments Ltd., UK), by using a disposable polystryrene cuvette (SARSTEDT AG & Co., Germany), whereas zeta potential (ZP) was measured by ELS using a disposable folded capillary cell (DTS1070, Malvern, UK) with the same instrument. Prior to the experiments, which were all conducted in triplicate, the NP were dispersed in an aqueous solution (Milli-Q-water, pH 8.0). The aforementioned techniques were applied in the physicochemical characterization of bare, conjugated (n=5) and non-conjugated (n=5), and drug-loaded, conjugated (n=3) and non-conjugated (n=3), NP.

3.3.2. MORPHOLOGY

The morphology of the NP was evaluated by TEM (Jeol JEM-1400, Jeol Ltd., Japan). For this purpose, samples were dispersed in aqueous solution (Milli-Q-water, pH 8.0) and a drop of the suspension placed on a carbon-coated copper grid (300 mesh; Electron Microscopy Sciences, USA) and left to dry at room temperature overnight.

3.3.3. CHEMICAL COMPOSITION

The chemical composition of PEG-functionalized and C1-loaded AcDexSp NP was studied with a Fourier-transform infrared spectroscopy (FTIR) spectrometer (Bruker Optics, Germany) and an attenuated total reflectance (ATR) sampling accessory (MIRacle, Pike Technology, Inc.). The ATR-FTIR spectra were recorded in the wavenumber region of 4000-650cm^{-1} with a resolution of 4cm^{-1}, at room temperature, using OPUS 5.5 software (Bruker, USA).

3.3.4. BEHAVIOR UNDER PHYSIOLOGICALLY RELEVANT pH-CONDITIONS

The behavior under physiologically relevant pH-conditions was accessed for AcDexSp and AcDexSp-PEG NP. Both types were individually added, at a concentration of 1mg/mL, into the buffer solutions - pH 7.4 and 5.0, to simulate the extracellular and intracellular environment, respectively. At different time points, samples (100μl) were withdrawn and immediately treated with a triethanoloamine (TEA) solution (0.01% v/v; 1mL, pH 8.0) to terminate the degradation process of the polymer. These samples were then centrifuged (16100*g*, 5min) and redispersed in the TEA solution. TEM imaging was performed as described in section 3.3.2.

3.3.5. DRUG RELEASE

The *in vitro* release of C1 drug from the nanocarriers was carried out under physiologically relevant pH-conditions – with two buffers: phosphate buffer saline (PBS) (pH 7.4) and acetate buffer (AB) (pH 5.0), to simulate the extracellular and intracellular environment, respectively. The drug-loaded NP were immersed in the appropriate release medium and stirred (150rpm) at 37±1°C. Free C1 served as control. For each test, samples of 200μl were taken at specific time points (2, 5, 10, 20, 30, 60, 120, 180, 360 and 1440min) and the same volume of preheated fresh medium was added back to maintain the final volume constant during the release experiment.

The samples were then centrifuged (16100*g*, 3min) and the supernatants collected for drug content quantification by HPLC as described in section 3.1. For the PBS, the standard plot mentioned in section 3.1. was used. Conversely, for the AB, a standard plot of the drug, using acetate as solvent, was generated over the concentration range of 0.05-50μg/mL and was found to be linear with r^2 value of 0,9999.

After the regular procedure concerning NP production, the exact volume of the suspension was measured and the content divided between two Eppendorf tubes. This step was then repeated resulting in a total of four Eppendorf tubes with the same approximate amount of NP. Next, centrifugation (16100*g*, 5min) was performed, the supernatants removed and the pellets kept within the Eppendorf tubes, which were placed in the oven, at 40°C, and left to dry overnight. Afterwards, the samples were weighted, being as the weight of their respective empty Eppendorf tube had already been taken. Three of the samples were

employed in the release assay. The other one was used to determine the LD (as described in section 3.1.), so that the volume of the buffer could be estimated in order to ensure sink conditions.

This *in vitro* release assessment was executed in triplicate and the corresponding data are represented as mean ± standard deviation.

3.3.6. STABILITY IN CELL MEDIUM

The colloidal stability of the NP was evaluated in Dulbecco's modified eagle medium (DMEM) medium containing 10% of fetal bovine serum (FBS). Briefly, the NP (500μg) were dispersed in 1mL of CCL for 2h under stirring (300rpm) at 37±1°C. At the following time points: 5, 10, 30, 60, 90 and 120 min, samples of 200μl were withdrawn and diluted 5x in Milli-Q-water (pH 8.0) for DLS and ELS measuring. This procedure was performed for AcDexSp (n=3) and AcDexSp-PEG (n=2) NP and the corresponding data are represented as mean ± standard deviation.

3.1.7. CYTOCOMPATIBILITY STUDIES

In the cellular viability (CV) studies, H9c2(2-1) (ATCC® CRL-1446™) embryonic rat heart-derived (ventricular) cells (myoblasts) were used because they have been widely used models for mimicking the response of primary cardiomyocytes to cardiac diseases (99–101).

The cells were seeded at densities of $1x10^4$ cells/well in 96-well plates (Corning, USA) and allowed to attach overnight. Afterwards, treatment of the cells ensued with a serial of concentrations of both bare and drug-loaded NP (25, 50, 100, 250, 500 and 1000μg/mL) in the CCM. After incubation, during 3 and 24h at 37°C, the plates were brought to room temperature for 30min and washed twice with Hank's Balanced Salt Solution (HBSS-HEPES, pH 7.4). Next, the plates were shaken for 2min after the addition of the assay reagent (CellTiter-Glo®, Promega, USA). The luminescence (LS) was measured in a Varioskan Flash Multimode Reader (Thermo Fisher Scientific), based on the principle that the ATP content of the cells is directly proportional to the CV, calculated by Eq. (3). Cells incubated in CCM, in Triton X-100 (1%) and in assay reagent were used as positive, negative and blank controls, respectively.

$$Cell\ viability\ (\%) = \frac{(LS\ of\ the\ treated\ cells - LSof\ the\ blank\ control)}{(LS\ of\ the\ positive\ control - LS\ of\ the\ blank\ control)} \times 100 \quad (3)$$

All these experiments were executed in triplicate. The levels of significance, assessed against the positive control, were evaluated by the Student's *t*-test and the probabilities set at *p <0,05, **p <0,01 and ***p <0,001.

4. RESULTS AND DISCUSSION

4.1. NANOPARTICLES PREPARATION

ORGANIC SOLVENT TYPE

As shown in Fig. 4, the results in terms of size, PDI and ZP were quite similar for both solvents. Despite this, the TEM observations revealed some differences between the two.

The NP prepared with DCM are spherical and more uniformly sized, while the use of EtOH provides NP which appear to be partly collapsed. The disparity, between DLS and TEM, may be attributed to the fact that while the TEM technique measures NP in a dry state, DLS does it in an aqueous environment (55,102).

The above could be explained by DCM's high immiscibility with water, low boiling point and high saturated vapor pressure which guarantee a high solvent evaporation rate. EtOH, conversely, is miscible with water, so there is a higher flux of solvent from the inner oil phase towards the external aqueous phase, which disturbs the solidification step and hence the final structure (36,102).

For the technique of encapsulation by an oil/water single emulsion and solvent evaporation, a suitable organic solvent must be able to dissolve both the chosen polymer (AcDexSp) and drug (C1), be immiscible in the aqueous phase and also have a high volatility, a low boiling point and low toxicity, as is the case for the two solvents employed. The advantage of using another organic solvent, instead of DCM, is related to toxicity. DCM is confirmed carcinogenic according to EPA data and so great efforts have been made to find a less toxic replacement, such as EtOH. However, DCM is still the most used for hydrophobic drug encapsulation with solvent evaporation technique, as established in the present study (36).

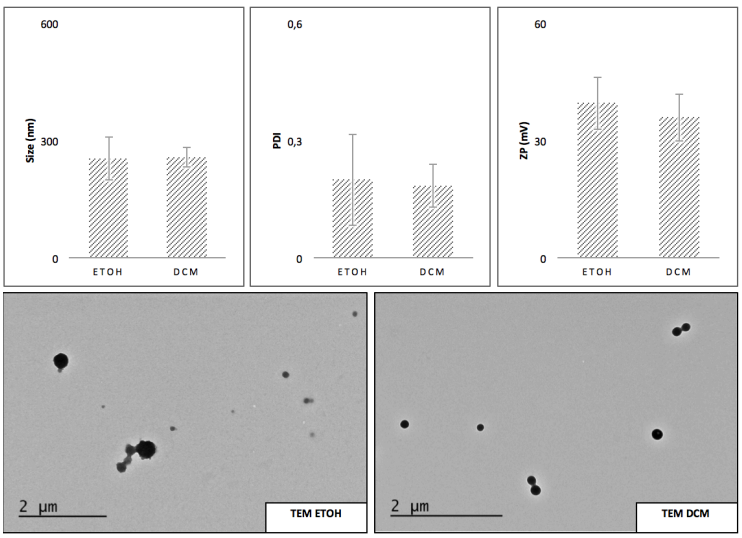

Fig. 4 - DLS, ELS and TEM for the NP prepared with EtOH and DCM

SURFACTANT CONCENTRATION

As can be seen (Fig. 5), the ZP results were approximately the same regardless of PVA varying concentrations, since a non-ionic surfactant was employed.

A decrease in both size and PDI of the NP was verified with increasing PVA concentration. One might infer that the amount of surfactant plays a critical role in both size and size distribution. In fact, smaller nanodroplets have larger surface areas and thus require more surfactant to stabilize the emulsion. Less surfactant, on the other hand, results in the formation of less stable emulsions with NP larger in size and PDI. It is therefore (37,103–106).

A decrease in EE was observed with increasing PVA concentration. When surfactant concentration reaches the critical micelle concentration, further addition of PVA will arrange as micelles instead of additionally reducing the surface tension. Bearing this in mind, with a greater amount of PVA, the C1 drug, being hydrophobic, may tend to diffuse out from the oil nanodroplets and solubilize as micelles in the aqueous phase (36,37).

Subsequently, a compromise ought to be reached between the lower size and PDI and highest EE and so the 2,5% concentration of PVA was selected.

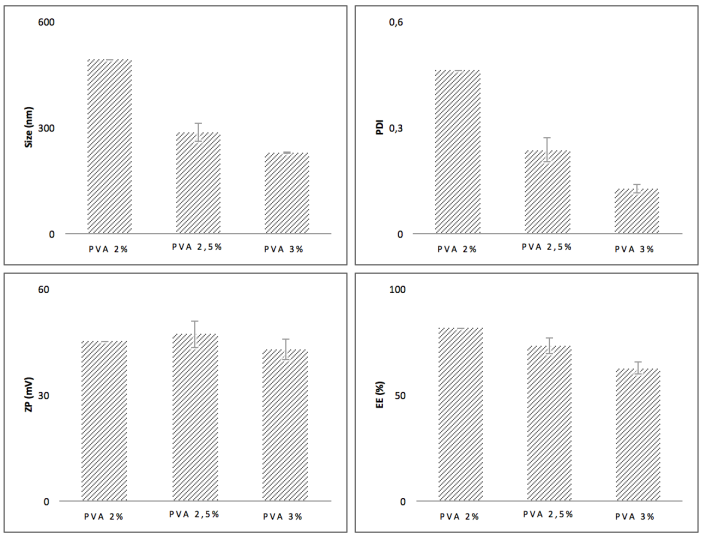

Fig. 5 - Size, PDI, ZP and EE for the varying concentrations of PVA

POLYMER AMOUNT, EVAPORATION TIME AND AQUEOUS PHASE VOLUME

As is evident from bellow (Fig. 6), doubling the amount of polymer while simultaneously altering the evaporation step – by increasing the time and reducing the volume of the aqueous phase – has no significant effect in terms of size, PDI and ZP. In spite of this, the previously mentioned condition is ideal for the formulation in question, due to the improvement in EE.

Upon decreasing the aqueous phase volume, better EE is achieved because less amount of drug is both lost and dissolved in the aqueous phase (107).

During solvent evaporation, two main mass transfers take place: solvent diffusion and its later evaporation into the air, which means that the oil nanodroplets - with the solvent

removal - become rich in polymer, begin to solidify and transition into NP. When evaporation is carried out for a shorter period of time, the diffusion of the organic solvent out of the oil phase may not have been complete before hardening of the nanodroplets occurs. On the contrary, if the organic solvent is allowed to evaporate for a longer time a greater extent of diffusion and evaporation of the solvent is ensured with enhanced outcomes in EE (36,37).

Increasing the polymer amount increases the viscosity of the inner oil phase, providing an enhanced diffusional resistance to drug loss, thereby entrapping more drug molecules in the polymer NP and conveying a higher EE. Another reason might be that the time required for polymer precipitation decreases at higher polymer concentration, so there would be less time for drug to diffuse out. Yet another possible reason could be related to the unsaturation of encapsulation, as there is a larger amount of polymer to encapsulate the same amount of drug (108–110).

It should be mentioned that although the effect of the polymer amount in varying the viscosity of the oil phase is commonly taken into account, the viscosity of the aqueous phase is rarely modified as it is very close to that of the water (36,111).

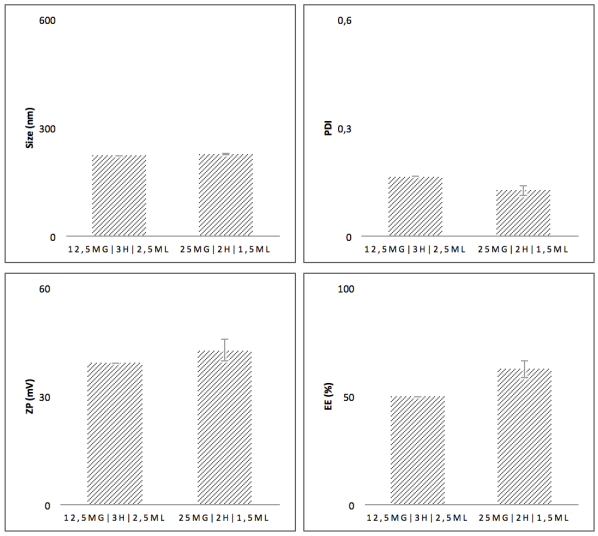

Fig. 6 - Size, PDI, ZP and EE comparison for the two conditions

DRUG QUANTITY

As demonstrated (Fig. 7), one might imply that the quantity of drug is not the key fundamental principle to define any of the NP' characteristics. The LD, in contrast, is obviously proportional to the quantity of drug used in the experiment.

Initially, the 4mg possibility was carried out but quickly changed to 1 mg as an attempt to improve conjugation with PEG. In attributing the difficulty of PEG-functionalization to the C1 incomplete encapsulation, lowering its fraction would improve the chance of the drug being entrapped within the polymer matrix instead of adsorbed onto the surface of the NP.

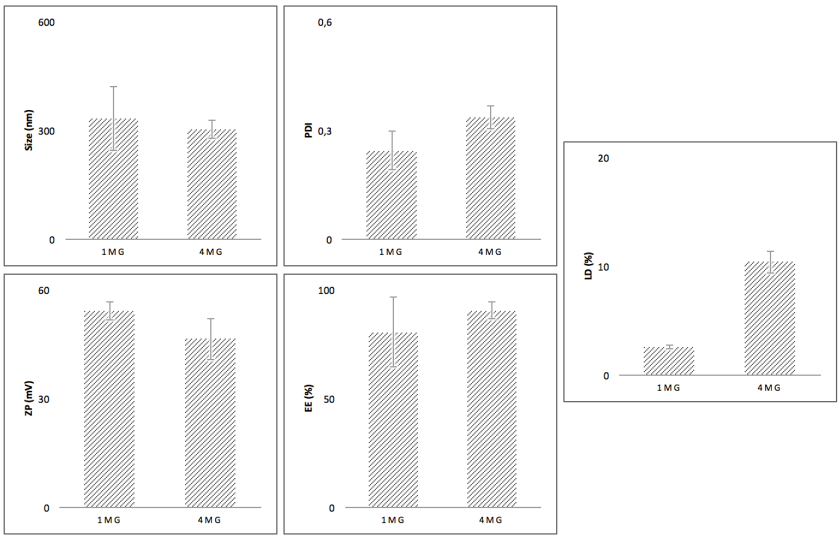

Fig. 7 - Characteristics of the NP with the two tested fractions of C1

4.2. NANOPARTICLES FUNCTIONALIZATION

pH

Although optimal activation of the carboxyl groups is given in acid conditions (pH 4.5-6.5), the polymer (AcDexSp) is acid-sensitive and so the final pH of the crosslinking solution must be at least 7.0, hence the two protocols evaluation (72,112).

The results in terms of size, PDI and ZP (Fig. 8) were relatively the same, suggesting that the carboxyl activation additional step brings no substantial advantage. Slightly acidic pH is ideal for the PEG's carboxyl groups activation, though neutral pH also provides them in sufficient amount in the protonated form so they are ready to participate in the EDC/NHS coupling chemistry.

Theoretically, to settle the conjugation, a basic pH should be favored since the spermine's amine groups, present in the surface of the NP, are of high pKa. The pKa values for free spermine's primary and secondary amines have been reported to be 10,1 and 10.9 and 8.0 and 8.8, respectively. This, in turn, at pH 7.0, entails the presence of protonated amino groups and hence with not as strong nucleophilic capability. That being said, the relevance of neutral pH lies with the Sulfo-NHS ester poor stability. In fact, the Sulfo-NHS ester revealed to be stable in acidic and neutral pH solutions but lost reactivity in basic solutions due to spontaneous hydrolysis (72,113,114).

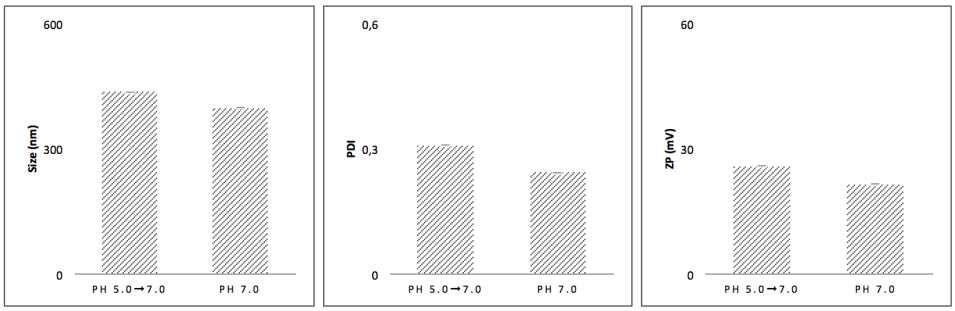

Fig. 8 - Size, PDI, and ZP for the two protocols

NP: PEG RATIO AND REACTION TIME

As might be seen (Fig. 9), there are no major differences for the two time points and thus the four-hour reaction was preferred to assure the NP' complete reaction within the Sulfo-NHS ester stability time frame, which is reported to be of only just a few hours at physiological pH (72,112).

As for the NP: PEG ratio, the DLS and ELS methods were not enough to deliver any indication about the optimal ratio. Further characterization with the FTIR (data not shown) established the impossibility of drawing conclusions, as the supposedly created amide bond, which embodies the functionalization proof, was not evidently apparent in the FTIR spectra for the ratios which were evaluated in this optimization attempt. It was then decided to increase the NP: PEG ratio to 1:10, in order to warrant visual confirmation in the form of the typical amide bands.

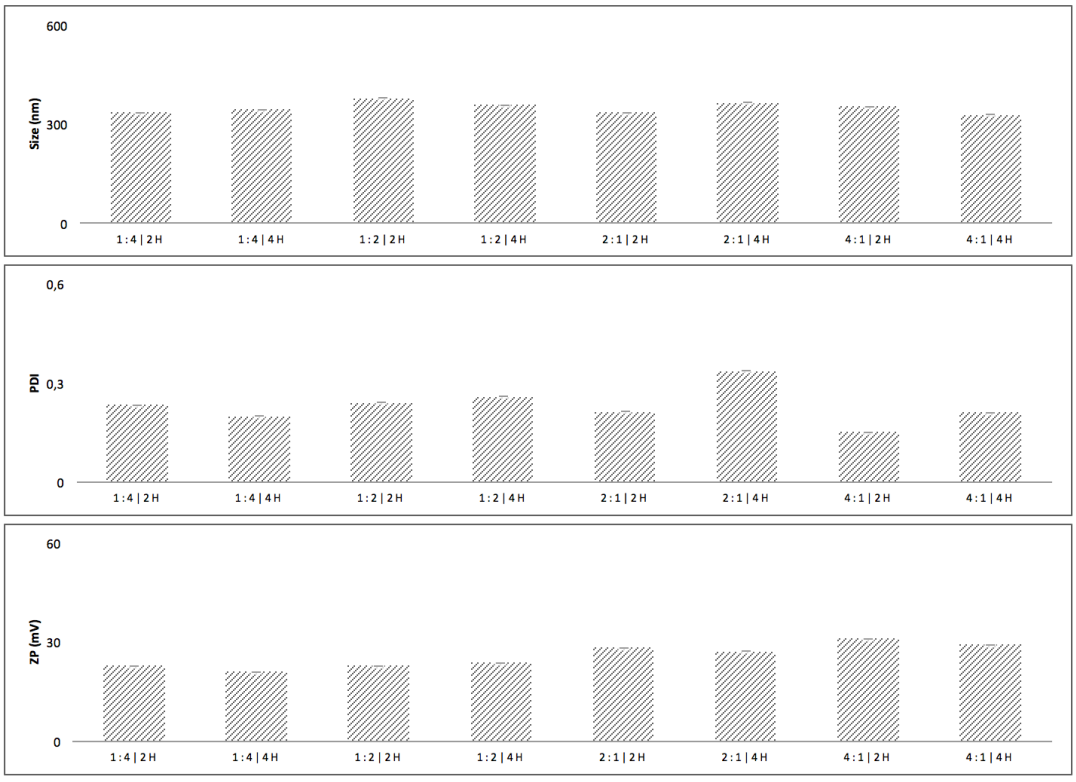

Fig. 9 - Size, PDI, and ZP for the different time points and NP: PEG ratios

PHYSICAL ADSORPTION

The disparity in ZP stands out over Fig. 10 analysis. The lower ZP has to do with functionalization, more precisely, with the presence of negatively charged carboxyl groups at the end of PEG molecules and the occupancy of the spermine's amine groups, both decreasing the overall NP positive charge - due to the cationic nature of AcDexSp. This implies the non-specifically adsorbed PEG removal from the surface of the NP during the washes and goes to show that covalent coupling assembles a stronger bond and a more stable conjugate than ionic adsorption (115–118).

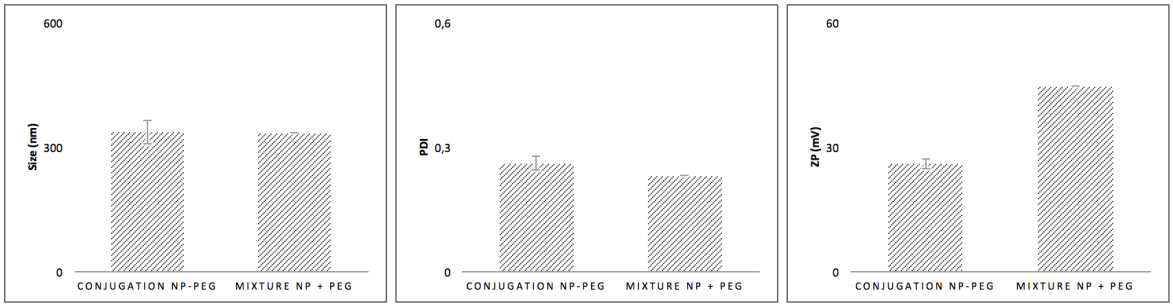

Fig. 10 - Size, PDI, and ZP for the PEG/NP mixture versus conjugation

4.3. NANOPARTICLES CHARACTERIZATION

4.3.1. SIZE, PDI AND ZP

As depicted in Table 4, no meaningful changes in particle size were detected in the PEG-functionalization step for bare NP, suggesting minimal particle decomposition under the reaction conditions. In fact, the slight increase in size may be attributed to the presence of PEG in the NP' surface. On the other hand, for drug-loaded NP, the size massively increased with PEG-functionalization, indicating colloidal instability.

All types of NP demonstrated a relative homogeneous size distribution with a PDI <0.3.

Bioconjugation was corroborated by the change in ZP for the bare NP – from 44,1 to 26,3, that is. However, one must point out the ZP contrast between the pairs of conjugated and non-conjugated NP: while AcDexSp and C1@AcDexSp NP displayed similar results, the alteration from AcDexSp-PEG to C1@AcDexSp-PEG NP supports the notion that aggregation might have occurred.

Although not clear how, something to do with the surface of the NP could somehow be the cause for obtaining increased-size NP and so an optimized functionalization was not achieved. In fact, the present of C1 in the supernatant kept from the last wash (data not shown) entails that the drug incomplete encapsulation within the polymer matrix, in other words, parts of C1 might have been in the surface of the NP rather than completely covered by the polymer matrix and hence preventing conjugation.

Table 4 - DLS and ELS for the different types of NP

	AcDexSp	*C1@AcDexSp*	*AcDexSp-PEG*	*C1@AcDexSp-PEG*
Size (nm)	272 ± 33,9	298 ± 84,9	322 ± 26,5	838 ± 38,5
PDI	0,24 ± 0,03	0,23 ± 0,06	0,25 ± 0,02	0,16 ± 0,01
ZP (mV)	44,1 ± 11,1	50,0 ± 4,90	26,3 ± 1,07	9,50 ± 2,16

4.3.2. MORPHOLOGY

The low magnification TEM images (Fig. 11) illustrate spherical and reasonable homogenously sized nanosystems, in accordance with the earlier obtained results concerning narrow size and its distribution. As a matter of fact, with regard to TEM imaging, the gradual size increase is fairly perceived from AcDexSp to C1@AcDexSp and, even more, from the former and the latter to AcDexSp-PEG NP.

It is also possible to deduce that bare NP functionalization has no obvious effect on the morphology, since the nanosystems retained their structure.

TEM analysis was not performed for C1@AcDexSp-PEG NP given that, within the arranged time period set for this study, conjugation was not managed to be optimized in terms

of their size which suggested aggregation. In *in vitro* testing, aggregates may lead to misrepresentative results and impairment of experimental reproducibility since, for instance, both cellular uptake and cytocompatible profile might be biased. Likewise, in *in vivo* administration, aggregation will lead to rapid clearance by the reticuloendothelial system, with the possibility of entrapment in the liver or the lungs due to capillary occlusion, thereby limiting the chance for NP to reach their therapeutic targets (119–122).

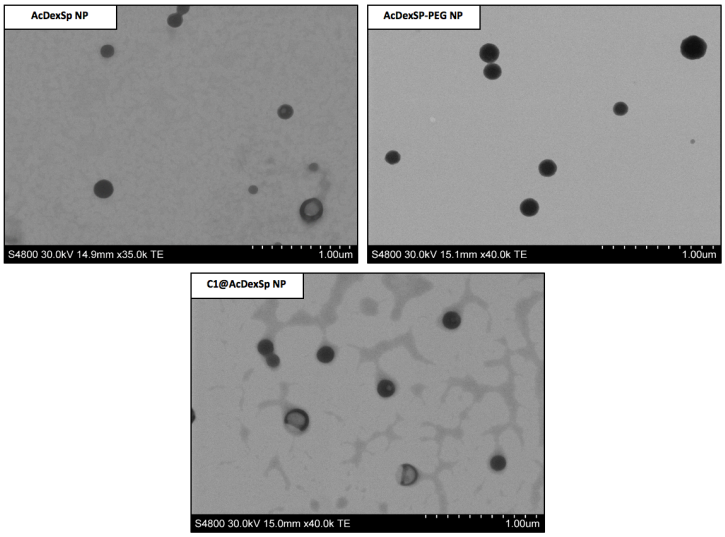

Fig. 11 - TEM for the different types of NP

4.3.3. CHEMICAL COMPOSITION

Analysis of PEG, AcDexSp NP and AcDexSp-PEG NP infrared spectra (Fig 12.) confirms PEG-conjugation. The appearance of amide-indicative bands at 1565-1570cm^{-1} (amide II: in plane N-H bending and C-N stretching - marked in dark blue) and 1630-1640cm^{-1} (amide I: amide C=O stretching - marked in light blue) represents the formation of a covalent amide bond, whereas the appearance of a shoulder at 1735cm^{-1} (C=O stretching from –COOH - marked in grey) denotes the presence of free carboxyl groups.

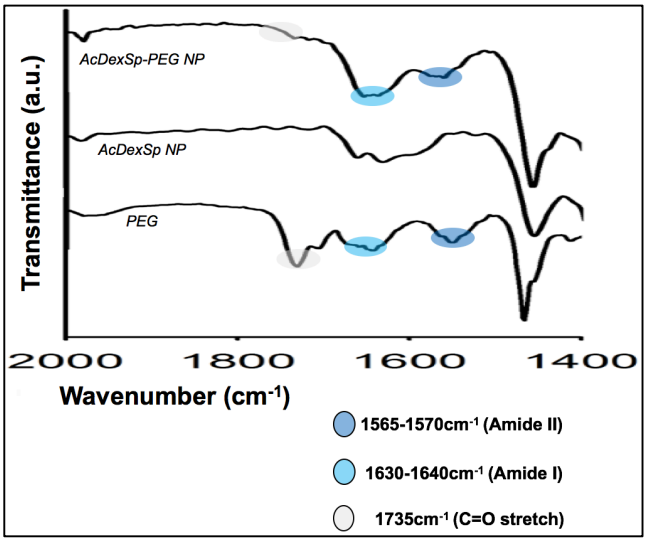

Fig. 12 - ATR-FTIR spectra of PEG, AcDexSp NP and AcDexSp-PEG NP

4.3.4. BEHAVIOR UNDER PHYSIOLOGICALLY RELEVANT pH-CONDITIONS

As can be observed, in Fig. 13, both types of NP maintained their structural integrity for up to 2h, at either value of pH. From that time point onwards, dissolution of the polymer matrix ensued, albeit with different rates for both types of NP and values of pH.

The degradation rate seems to be faster at pH 5.0, with the nanocarriers complete disappearance after 28h. This upholds the notion that AcDexSp decomposes in mild acidic conditions, being classified as an acid-sensitive polymer. It should be mentioned that functionalized NP appeared to have higher degradation rate than their non-conjugated counterparts.

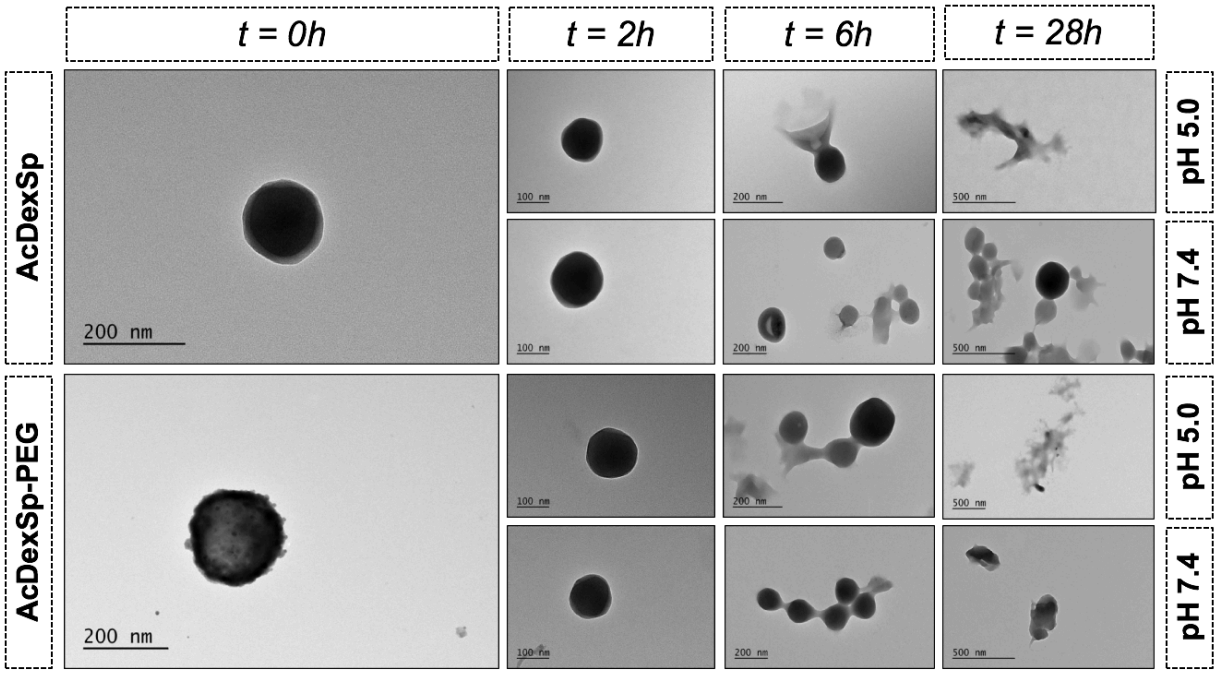

Fig. 13 - Behavior of AcDexSp and AcDexSp-PEG NP at pH 5.0 and 7.4

4.3.5. DRUG RELEASE

First, in Fig. 14, the partial resemblance between the free drug dissolution profile and the drug-loaded NP release one (either PEGylated or not), in their respective dissolution medium, indicates that both their release is only to a certain extent dictated by the degradation rate of the outer AcDexSp matrix.

If one compares the three-colored curves in account to the percentage of released drug, at the 30min time point, at pH 5.0 it decreases from 87% (control) to 24 (C1@AcDexSp) and 50% (C1@AcDexSp-PEG) and at pH 7.4 it goes from 30% (control) to 3 (C1@AcDexSp) and 15% (C1@AcDexSp-PEG). It appears that in the beginning, both types of NP, conjugated or not, restrain C1 dissolution, although this sustained release is clearly prolonged at pH 7.4 as evident from the same comparison applied to the last time points. It is reported that this relatively small burst with sustain release suggests that most of C1 was indeed entrapped in the core of the NP rather than weakly bound or adsorbed in the surface (81,88,123–125).

Release being much faster at pH 5.0 is, on one hand, in accordance with the drug higher solubility at this value of pH, as is clear from C1 dissolution curves comparison, in which the drug exhibits a burst dissolution profile (73% of drug dissolved after 2min) at this value of pH. On the other hand, it also fairly corroborates the polymer pH-responsive properties, already detailed (in section 4.1.4.), and underlines the concept that a higher degradation of the polymer matrix will pave the way to a faster drug release.

The release kinetics and mechanism of C1 was evaluated by plotting the release data into various mathematical models including zero-order, Higuchi, Hixson-Crowell and Korsmeyer-Peppas (Table 1). The linear regressions are summarized in Tables 5 and 6, where R^2 is the squared correlation coefficient, k is a rate constant and n is the release exponent.

The analysis of drug release mechanism was performed in regard to the different release exponents (Table 3), with values of n indicating that all NP released C1 through the cooperative processes of diffusion and erosion. Despite this, diffusion is most certainly the predominant mechanism, since after the release media penetration and drug dissolution, C1 diffuses through the small porous already existent in the polymer matrix or the channels which are being formed with the help of erosion (82,86,87,126,127).

The exception for the above lies with C1@AcDexSp-PEG NP at pH 5.0. The logical explanation is that adding up to higher degradation rate of AcDexSp at pH 5.0, the presence of PEG provides the NP a hydrophilic surface that enables water penetration into the polymer matrix, which accelerates the degradation process in such way that matrix erosion becomes faster than drug diffusion (81,126,127).

On the basis of the best fit model with the highest R^2, the results, as expected, are in line with the ones above, given that the kinetic model leads the mechanism of drug release. For pH 7.4 and for C1@AcDexSp NP at pH 5.0, the kinetic of C1 release was best expressed by Higuchi's model where the diffusion of the drug is proportional at the square root of time. For C1@AcDexSp-PEG NP at pH 5.0, conversely, the kinetic of C1 release was best expressed by Hixson-Crowell's model where the release of the drug is erosion-dependent and so proportional to the surface area of the nanosystem (82,87).

On a side note, the interference of the NP drying step must not be neglected, since it may have meddled with the polymer solid-state. It is reported that crystalline polymer matrices have rough surfaces with large surface areas, unlike amorphous polymer matrices which are just the opposite. The former results in reduced release whereas the release from the latter is much larger because a smoother and smaller surface has greater porosity. Temperature is a process engineering aspect that should be carefully tampered with since drawbacks of its elevation are quite a few, from decreasing of EE to the morphology becoming coarser and, if too high, disnature of the drug might arise (36,37,110,128).

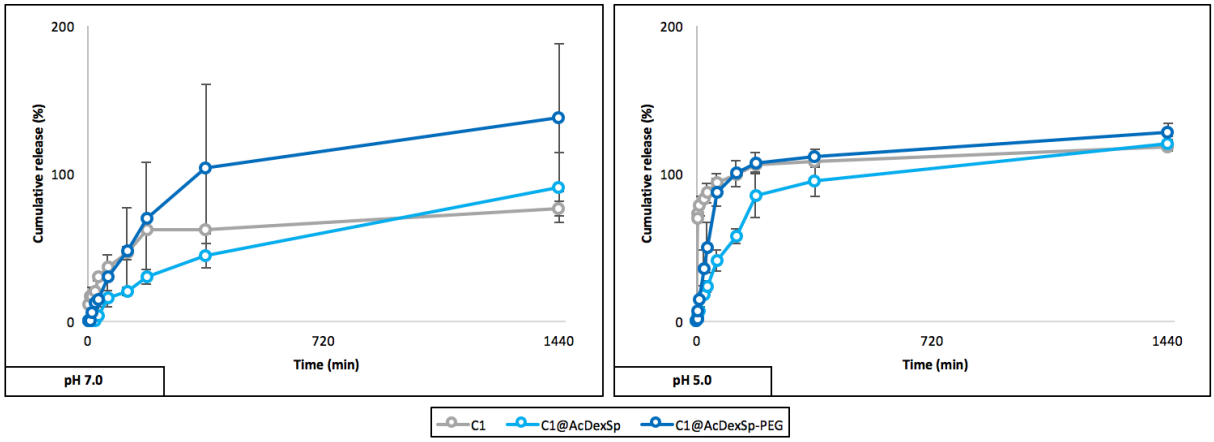

Fig. 14 - Drug release of C1, C1@AcDexSp and C1@AcDexSp-PEG at different pH conditions

Table 5 - Release mechanism of C1 from the NP at different pH conditions

		pH 5.0		pH 7.0	
		C1@AcDexSp	*C1@AcDexSp-PEG*	*C1@AcDexSp*	*C1@AcDexSp-PEG*
Korsemeyer-Peppas	R^2	0,989	0,992	0,758	0,946
	n	0,841	1,114	0,683	0,847
	K_{kp}	0,867	0,837	0,403	0,599

Table 6 - Release kinetics of C1 from the NP at different pH conditions

		pH 5.0		pH 7.0	
		C1@AcDexSp	*C1@AcDexSp-PEG*	*C1@AcDexSp*	*C1@AcDexSp-PEG*
Zero-order	R^2	0,617	0,405	0,906	0,739
	$k_0 \times 10^{-3}$	57,00	53,80	63,10	94,50
Higuchi	R^2	0,866	0,934	0,987	0,934
	$k_h \times 10^{-3}$	2609	2987	2546	2987
Hixson-Crowell	R^2	0,768	0,245	0,957	0,982
	$-k_{hc} \times 10^{-3}$	1,600	1,800	1,000	3,200

4.3.6. STABILITY IN CELL MEDIUM

Bearing in mind that in *in vitro* systems NP may interact with components of the cell culture prior to any cellular contact and that cell media complexity may affect such interactions, it became imperative to access their colloidal stability in the protein-supplemented and electrolyte enriched CCM (129–131).

In Fig. 15, the increase of size and PDI over time is visible for AcDexSp NP, whereas for the PEGylated NP, these two parameters remained constant throughout the test time

points. In either case, the surface charge dropped to ≈(-)16mV because ZP was measured in DMEM with 10% of FBS, which is rich in negatively charged molecules (proteins) (129).

As soon as NP are dispersed in the medium adsorption of proteins occurs. The low colloidal stability of the non-conjugated NP is explained by the favorable interaction between the positively charged amino groups on the surface of the NP and the negative charge of this proteins. Consequently, the electrostatic stabilizing repulsive forces decrease in favor of the van der Waals destabilizing attractive ones and thus aggregation succeeds. Actually, numerous studies have shown that protein adsorption plays a prominent role regarding NP' stability and their interaction with biological systems (132–137).

In contrast, the PEG-functionalization prevents the formation of destabilizing attractive van der Waals interactions by steric stabilization, that is, by increasing the steric distance between NP. As a matter of fact, surface modification, and subsequent steric stabilization, is the most generally acknowledged approach to improve colloidal stability. Moreover, PEGylation entails more hydrophilicity via ether repeats forming hydrogen bonds with the solvent. It has been demonstrated that PEG, a well investigated and widely used polymer in the field, can reduce protein adsorption and act as a physical barrier to block NP aggregation (64,119,138–140).

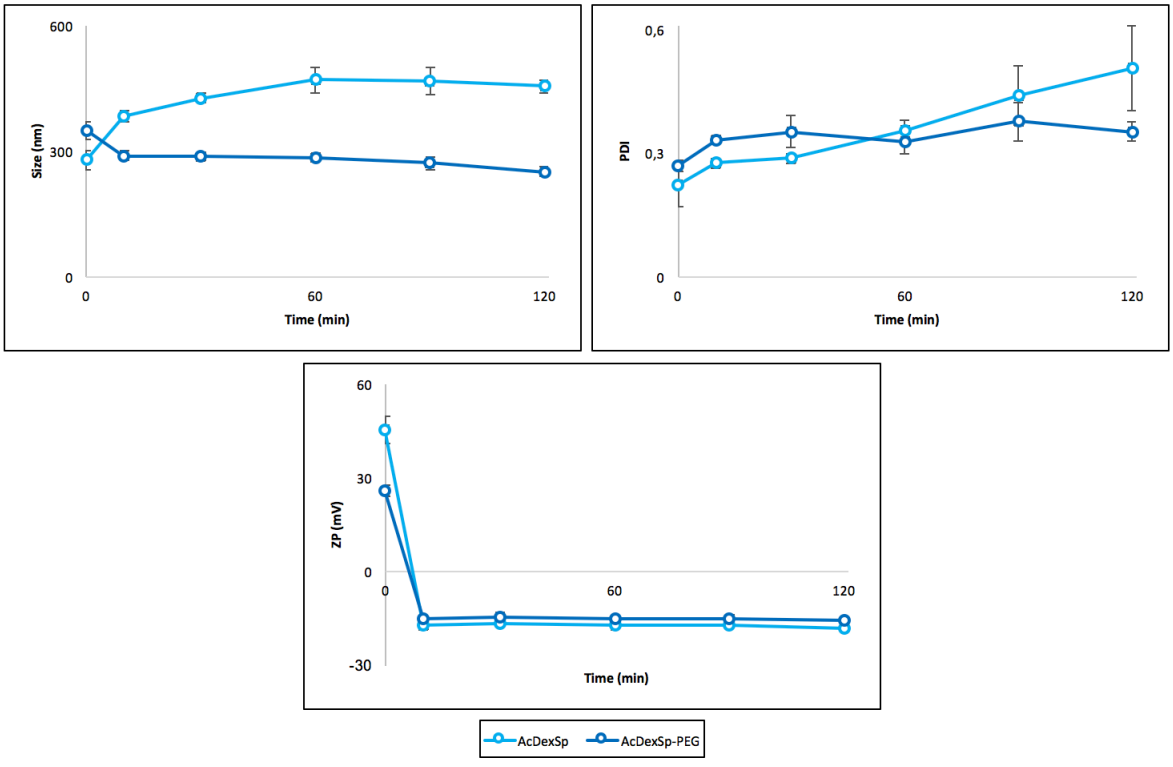

Fig. 15 - Stability of AcDexSp and AcDexSp-PEG NP

4.3.7. CYTOCOMPATIBILITY STUDIES

In Fig. 16, one may verify that, at the three-hour time point, for all types of NP, the CV was close to 100%. Inversely, at the twenty-four-hour time point, the functionalized NP

remained non-cytotoxic for concentrations up to 1000μg/mL, whereas the non-conjugated ones presented dose-dependent CV: the number of viable cells dropped from ≈90 to ≈50% with rising NP concentration.

Cytotoxicity depends, among other factors, on cellular uptake, which, in turn, is essentially governed by size, hydrophobicity and charge. In order to reach conclusions about surface effects (hydrophobicity and charge, that is), one must not neglect the importance of size. In this study, comparisons were valid given that the size of the NP in question was reasonably similar.

The lower cell CV of AcDexSp and C1@AcDexSp NP is due to the presence of the positively charged spermine's amine groups. In fact, cationic NP cause more pronounced disruption of plasma membrane integrity, stronger mitochondrial and lysosomal damage and a higher number of autophagosomes (141).

The higher cytocompatibility of PEGylated NP, besides its intrinsic hydrophilic nature, may be attributed to the lower level of cell uptake and so PEG was able to shield NP interaction and reduce cell killing. It has actually been reported that PEG coating can significantly decrease unspecific intracellular uptake. Also reported is the shielding of cationic groups by PEGylation which decreased both cytotoxicity and efficacy linked to positive charge (54,115,142,143).

It appears that C1 drug has no noteworthy effect concerning CV, since no different outcome was detected when comparing bare and drug-loaded NP.

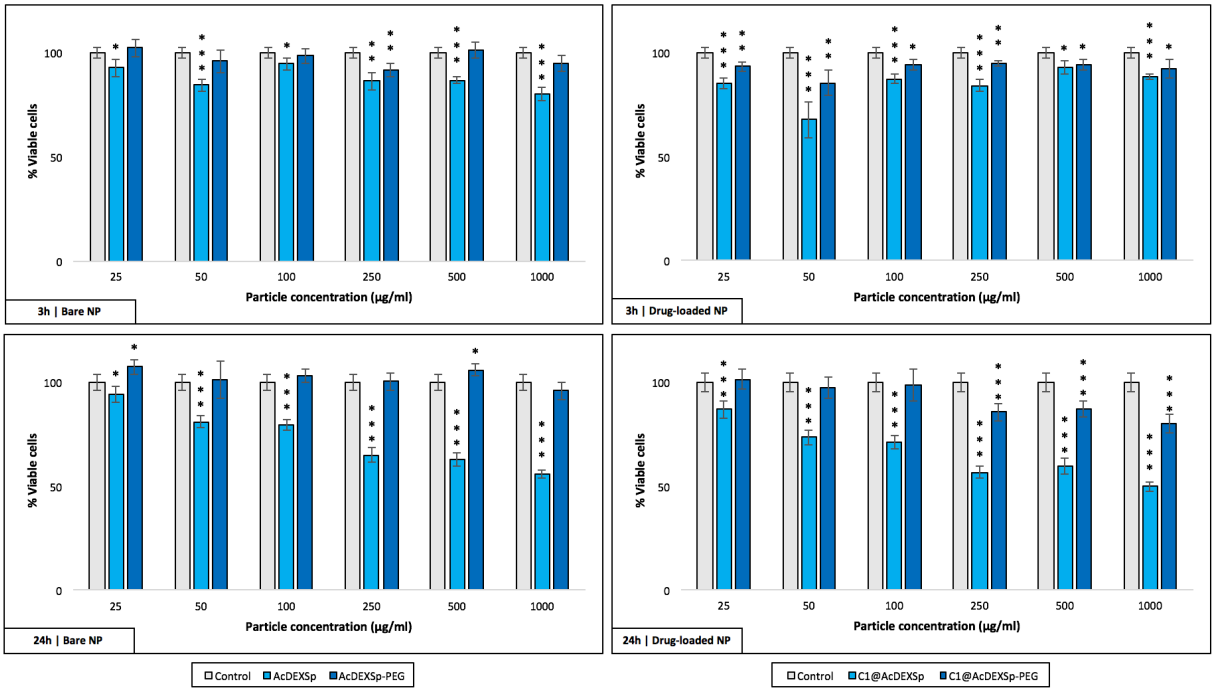

Fig. 16 - CV studies for the different types of NP

5. CONCLUSIONS AND FUTURE PERSPECTIVES

5.1. CONCLUSIONS

The main conclusions of the present dissertation are resumed as follows:

- Process and formulation variables can be effectively altered while aiming to achieve the desired NP characteristics. In this investigation, the best combination of said variables was determined to be with DCM as organic solvent, an intermediate concentration (2.5%) of surfactant, doubling the amount (25mg) of polymer, maximizing the evaporation time (3h) while minimizing the aqueous phase volume (1.5mL) and a small drug amount (1mg);
- In absence of standard conjugation protocols, each particular case (nanoparticle + biomolecule) requires optimization, since NP' functionalization is crucial to impart biological recognition and interaction skills. PEGylation was optimized to a four-hour time point and a ratio of 1:10 (NP: PEG);
- The impossibility of PEGylation for drug-loaded NP was never fully understood, due to ambiguous results: the presence of C1 in the last supernatant (indicating incomplete encapsulation) and the sustained release from the polymer matrix (entailing its presence at the core of the NP);
- Upon functionalization both stability and biocompatibility of the nanosystem improved. In this study, it has been established that cationic surface charge of the NP correlates with greater cytotoxicity and that PEG-conjugation reduces the adsorption of proteins to the NP' surface. In a broader context, understanding the factors that influence NP' colloidal stability and cytocompatibility when put in contact with biological media is paramount while aiming at the development of safe and effective nanotherapeutics for clinical use;
- One of the aims of the study focused on developing a nanosystem for pH-triggered drug delivery. On this note, a substantial difference in drug release should have been observed, more specifically, a sustained and burst release at neutral and acidic environment, respectively. This ensures that the cargo is only allowed to be released in the target tissue in response to intracellular acidification upon cellular uptake. The possible explanations for not obtaining such results are, most likely, related to the drug used in this study. C1 turned out to have a pH-dependent solubility, making extrapolations harder for the also pH-dependent polymer matrix degradation. Additionally, one must reinforce that C1 was not a truly poorly-water soluble drug.

5.2. FUTURE PERSPECTIVES

Some suggestions and considerations for upcoming studies are listed as follows:

- Aiming at boosting the change of conjugation, a new drug and organic solvent ought to be considered. This because C1 demonstrated to be quite hydrophilic (with a burst release in aqueous medium) and so, with a real hydrophobic drug and a less polar organic solvent (such as chloroform), one would guarantee drug confinement within the organic phase and, hence, within the polymer matrix, by avoiding its migration towards the surface of the NP.
- The possibility of carefully controlling the degradation rate of AcDexSp can be taken advantage of and, depending on the desired intent, may vary from minutes to months. It is therefore recommended the pursue of reaction time's effect on acetal coverage (47).
- MeOH is a well-known toxic for human health, so that it is metabolized to formic acid and subsequently leads to metabolic acidosis, blindness and death. Being a degradation product of AcDexSp, one must consider if high-frequency dosing would not result in the release of unsafe levels of said compound. The ensuing logical step would be the use of an AcDexSp-analog which has the much safer EtOH as one of its byproducts (47).
- In spite of the fact that the pH of the functionalization turned out to be irrelevant, not immediately triggering the quest for in-depth research, one must stress the critical need of an intensive investigation into the mechanisms of EDC/NHS coupling under various experimental conditions such as ratio (EDC: NHS), coupling time and buffer type (112).
- Several other factors should be reflected upon while designing a PEGylation protocol. In what PEG's chain length is concerned the goal is to improve circulation time, whether by using larger PEG molecules (with small NP) which prevent excretion and enhance recirculation, or smaller ones (with large NP) due to the further increase in size. Additionally, the PEG's terminus charge, either positive (amine) or negative (carboxyl) may come into play in phagocytic events (64).
- PEGylation of nanosystems may be extended to other drugs with short plasma half-life, low bioavailability and/or poor water solubility, since it can strategically overcome these delivery barriers. Nonetheless, one must mention that repeated injections of PEGylated material end up showing markedly decreased plasma half-life, which is thought to be related to increased splenic production of immunoglobulin M (64).
- As an alternative, besides ELS and FTIR, the successful functionalization could also had been confirmed through elemental analysis, where the amount of conjugated PEG per milligram of NP could be calculated by balancing the percentage of each chemical element and the chemical structure of PEG.
- In the behavior under physiologically pH-relevant conditions, supplementary digital photos of the nanocarriers, at different time points, might had been taken, in order to observe the transition from opaque suspension to transparent solution, when decomposition of the polymer matrix is completed (52).

- It is quite often verified that *in vitro* release studies do not correlate with *in vivo* release profiles. That happens because physiological conditions are much more complex than the buffer solutions commonly employed. For enhancing the accuracy of the evaluation, one may use simulated release media or design *in vivo* release models, albeit for this last alternative one should also consider the time, the cost and the fact that mathematical models, which can represent the real physiological conditions, have yet to be developed (80).
- The stability testing carried out in this investigation is rather limited. First, the protein levels of the CCM (DMEM with 10% of FBS) are approximately twenty times lower that in human plasma. Secondly, due to financial restraints, cell media suppliers only analyze certain components, not accessing the lipid content or other specific proteins. As a result, the different composition, when paralleling supplemented cell media and human plasma, impedes the direct extrapolation of data obtained *in vitro* to colloidal behavior of NP *in vivo* (129). Even if human plasma was used, there is another undermining factor, which is largely overlooked and has to do with the fact that physiological fluids are dynamic by nature, with blood moving at different speeds, ranging from a few micrometers per second (in the capillaries) up to sixty centimeters per second (in the ascending aorta) (12).
- The cytocompatibility studies would benefit with the addition of new types of cells, such as primary cardiomyocytes and non-myocytes (fibroblasts). Cardiomyoctes are major constituents of the mammalian heart. Fibroblasts, on the other hand, turn out to be a central type cell in the injured area during the post-MI healing phase. One might even mimic hypoxia by pretreating the cells with cobalt chloride prior to any CV experiments (144).
- The present study intended to use PEG as a spacer for further functionalization with a heart-homing molecule, which was not possible, due to time constrains. The first and foremost challenge in heart targeting is the lack of a specific cardiac marker. Keeping this in mind, Ferreira *et al.* worked with peptide-conjugated NP, more specifically, atrial natriuretic peptide (28 amino acid sequence: SLRRSSCFGGRMDRIGAQSGLGCNSFRY), P2 (9 amino acid sequence: CSTSMLKAC) and P3 (12 amino acid sequence: CRSWNKADNRSC), providing plenty of data for their future employment as nanovectors in MI and HF (145). Later on, Ferreira *et al.* went to show that atrial natriuretic peptide-functionalized NP accumulate into the endocardial region of the failing heart, where it is known for this molecule to be predominantly expressed (144).
- Despite the emerging advances in the field of nanoscience applied to cardiovascular disease, with reports of both *in vitro* and animal studies rapidly and steadily being published, their successful clinical translation remains elusive. In fact, of the enormous and growing arsenal of nanotechnology developed to date, few have reached clinical trials and even fewer have been approved for clinical use. One of the main issues is the mass

production of NP for clinical development and commercialization, due to the lack of reproducible manufacturing processes. Other shortcoming, explaining the huge gap between bench discoveries and clinical trials, is the biological identity of NP. When in contact with biological fluids, NP are quickly surrounded by a layer of proteins, the so-called protein corona, which defines their biological identity and which has not yet been properly addressed in the field of cardiac nanotechnology. One must then stress the concept of personalized therapy for designing safe and effective NP, given the inter and intra-patient variations in blood plasma composition (12).

- Overall, the present work provides a universal, biocompatible and functional platform for controlled intracellular nanodelivery, taking into account that this system could be suitable for the encapsulation of other bioactive compounds with potential applications in distinctive biomedical fields.

6. REFERENCES

1. Roger VL, Go AS, Lloyd-Jones DM, Benjamin EJ, Berry JD, Borden WB, et al. Heart Disease and Stroke Statistics--2012 Update: A Report From the American Heart Association. Circulation. 2012 Jan 3;125(1):e2–220.
2. Esper SA, Subramaniam K. Heart failure and mechanical circulatory support. Best Pract Res Clin Anaesthesiol. 2012 Jun 1;26(2):91–104.
3. Ho YT, Poinard B, Kah JCY. Nanoparticle drug delivery systems and their use in cardiac tissue therapy. Nanomedicine. 2016 Mar;11(6):693–714.
4. Go AS, Mozaffarian D, Roger VL, Benjamin EJ, Berry JD, Blaha MJ, et al. Heart Disease and Stroke Statistics--2014 Update: A Report From the American Heart Association. Circulation. 2014 Jan 21;129(3):e28–292.
5. Ziaeian B, Fonarow GC. Epidemiology and aetiology of heart failure. Nat Rev Cardiol. 2016 Mar 3;13(6):368–78.
6. Libby P, Ridker PM, Maseri A. Inflammation and atherosclerosis. Circulation. 2002 Mar 5;105(9):1135–43.
7. Nabel EG, Braunwald E. A Tale of Coronary Artery Disease and Myocardial Infarction. N Engl J Med. 2012 Jan 5;366(1):54–63.
8. Libby P, Ridker PM, Hansson GK. Progress and challenges in translating the biology of atherosclerosis. Nature. 2011 May 18;473(7347):317–25.
9. Xin M, Olson EN, Bassel-Duby R. Mending broken hearts: cardiac development as a basis for adult heart regeneration and repair. Nat Rev Mol Cell Biol. 2013 Jul 10;14(8):529–41.
10. Thygesen K, Alpert JS, Jaffe AS, Simoons ML, Chaitman BR, White HD, et al. Third Universal Definition of Myocardial Infarction. Circulation. 2012 Oct 16;126(16):2020–35.
11. Ferreira MPA, Balasubramanian V, Hirvonen J, Ruskoaho H, Santos HA. Advanced Nanomedicines for the Treatment and Diagnosis of Myocardial Infarction and Heart Failure. Curr Drug Targets. 2015;16(14):1682–97.
12. Mahmoudi M, Yu M, Serpooshan V, Wu JC, Langer R, Lee RT, et al. Multiscale technologies for treatment of ischemic cardiomyopathy. Nat Nanotechnol. 2017 Sep 6;12(9):845–55.
13. Santos CXC, Anilkumar N, Zhang M, Brewer AC, Shah AM. Redox signaling in cardiac myocytes. Free Radic Biol Med. 2011 Apr 1;50(7):777–93.
14. Talman V, Ruskoaho H. Cardiac fibrosis in myocardial infarction—from repair and remodeling to regeneration. Cell Tissue Res. 2016 Sep 21;365(3):563–81.
15. Adler ED, Goldfinger JZ, Kalman J, Park ME, Meier DE. Palliative Care in the Treatment of Advanced Heart Failure. Circulation. 2009 Dec 22;120(25):2597–606.
16. Chang M-Y, Yang Y-J, Chang C-H, Tang ACL, Liao W-Y, Cheng F-Y, et al. Functionalized nanoparticles provide early cardioprotection after acute myocardial infarction. J Control Release. 2013 Sep 10;170(2):287–94.
17. Suarez S, Grover GN, Braden RL, Christman KL, Almutairi A. Tunable Protein Release from Acetalated Dextran Microparticles: A Platform for Delivery of Protein Therapeutics to the Heart Post-MI. Biomacromolecules. 2013 Nov 11;14(11):3927–35.

18. Lowe HC, Neill BD Mac, Van de Werf F, Jang I-K. Pharmacologic reperfusion therapy for acute myocardial infarction. J Thromb Thrombolysis. 2002 Dec;14(3):179–96.

19. Ambrosy AP, Fonarow GC, Butler J, Chioncel O, Greene SJ, Vaduganathan M, et al. The Global Health and Economic Burden of Hospitalizations for Heart Failure. J Am Coll Cardiol. 2014 Apr 1;63(12):1123–33.

20. Torchilin VP. Targeted pharmaceutical nanocarriers for cancer therapy and imaging. AAPS J. 2007 Jun 11;9(2):E128–47.

21. Tölli MA, Ferreira MPA, Kinnunen SM, Rysä J, Mäkilä EM, Szabó Z, et al. In vivo biocompatibility of porous silicon biomaterials for drug delivery to the heart. Biomaterials. 2014 Sep;35(29):8394–405.

22. Eniola-Adefeso O, Heslinga MJ, Porter TM. Design of nanovectors for therapy and imaging of cardiovascular diseases. Methodist Debakey Cardiovasc J. 2012 Jan;8(1):13–7.

23. Galagudza M, Korolev D, Postnov V, Naumisheva E, Grigorova Y, Uskov I, et al. Passive targeting of ischemic-reperfused myocardium with adenosine-loaded silica nanoparticles. Int J Nanomedicine. 2012;7:1671–8.

24. Scott RC, Rosano JM, Ivanov Z, Wang B, Chong PL-G, Issekutz AC, et al. Targeting VEGF-encapsulated immunoliposomes to MI heart improves vascularity and cardiac function. FASEB J. 2009 Oct 1;23(10):3361–7.

25. Scott RC, Wang B, Nallamothu R, Pattillo CB, Perez-Liz G, Issekutz A, et al. Targeted delivery of antibody conjugated liposomal drug carriers to rat myocardial infarction. Biotechnol Bioeng. 2007 Mar 1;96(4):795–802.

26. Galagudza MM, Korolev D V, Sonin DL, Postnov VN, Papayan G V, Uskov IS, et al. Targeted drug delivery into reversibly injured myocardium with silica nanoparticles: surface functionalization, natural biodistribution, and acute toxicity. Int J Nanomedicine. 2010 Apr 7;5:231–7.

27. Zhang J, Zhang X, Li X, Zhao Y, Luo H, Pan W, et al. Core-shell hybrid liposomal vesicles loaded with panax notoginsenoside: preparation, characterization and protective effects on global cerebral ischemia/reperfusion injury and acute myocardial ischemia in rats. Int J Nanomedicine. 2012 Aug;7:4299.

28. Almer G, Frascione D, Pali-Schöll I, Vonach C, Lukschal A, Stremnitzer C, et al. Interleukin-10: An Anti-Inflammatory Marker To Target Atherosclerotic Lesions via PEGylated Liposomes. Mol Pharm. 2013 Jan 7;10(1):175–86.

29. Simón-Yarza T, Tamayo E, Benavides C, Lana H, Formiga FR, Grama CN, et al. Functional benefits of PLGA particulates carrying VEGF and CoQ10 in an animal of myocardial ischemia. Int J Pharm. 2013 Oct 1;454(2):784–90.

30. Paulis LE, Geelen T, Kuhlmann MT, Coolen BF, Schäfers M, Nicolay K, et al. Distribution of lipid-based nanoparticles to infarcted myocardium with potential application for MRI-monitored drug delivery. J Control Release. 2012 Sep 10;162(2):276–85.

31. Miyagi Y, Zeng F, Huang X-P, Foltz WD, Wu J, Mihic A, et al. Surgical ventricular restoration with a cell- and cytokine-seeded biodegradable scaffold. Biomaterials. 2010 Oct;31(30):7684–94.

32. Tiwari S, Verma P. Microencapsulation technique by solvent evaporation method (Study of effect of process variables). Int J Pharm Life Sci. 2011;2(8):998–1005.

33. Soppimath KS, Aminabhavi TM, Kulkarni AR, Rudzinski WE. Biodegradable polymeric nanoparticles as drug delivery devices. Vol. 70, Journal of Controlled Release. Elsevier; 2001. p. 1–20.

34. Berkland C, King M, Cox A, Kim K, Pack DW. Precise control of PLG microsphere size provides enhanced control of drug release rate. J Control Release. 2002 Jul 18;82(1):137–47.

35. Freiberg S, Zhu XX. Polymer microspheres for controlled drug release. Vol. 282, International Journal of Pharmaceutics. Elsevier; 2004. p. 1–18.

36. Li M, Rouaud O, Poncelet D. Microencapsulation by solvent evaporation: State of the art for process engineering approaches. Int J Pharm. 2008 Nov;363(1–2):26–39.

37. Sharma N, Madan P, Lin S. Effect of process and formulation variables on the preparation of parenteral paclitaxel-loaded biodegradable polymeric nanoparticles: A co-surfactant study. Asian J Pharm Sci. 2016 Jun;11(3):404–16.

38. Lawrence MJ, Rees GD. Microemulsion-based media as novel drug delivery systems. Adv Drug Deliv Rev. 2000 Dec;45(1):89–121.

39. Jeong B, Gutowska A. Lessons from nature: stimuli-responsive polymers and their biomedical applications. Trends Biotechnol. 2002 Jul;20(7):305–11.

40. Gao W, Chan JM, Farokhzad OC. pH-Responsive Nanoparticles for Drug Delivery. Mol Pharm. 2010 Dec 6;7(6):1913–20.

41. Kauffman KJ, Kanthamneni N, Meenach SA, Pierson BC, Bachelder EM, Ainslie KM. Optimization of rapamycin-loaded acetalated dextran microparticles for immunosuppression. Int J Pharm. 2012 Jan 17;422(1–2):356–63.

42. Bachelder EM, Beaudette TT, Broaders KE, Dashe J, Fréchet JMJ. Acetal-Derivatized Dextran: An Acid-Responsive Biodegradable Material for Therapeutic Applications. J Am Chem Soc. 2008 Aug 13;130(32):10494–5.

43. Cohen JL, Schubert S, Wich PR, Cui L, Cohen JA, Mynar JL, et al. Acid-Degradable Cationic Dextran Particles for the Delivery of siRNA Therapeutics. Bioconjug Chem. 2011 Jun 15;22(6):1056–65.

44. Davis ME, Chen Z (Georgia), Shin DM. Nanoparticle therapeutics: an emerging treatment modality for cancer. Nat Rev Drug Discov. 2008 Sep 1;7(9):771–82.

45. Dhar S, Kolishetti N, Lippard SJ, Farokhzad OC. Targeted delivery of a cisplatin prodrug for safer and more effective prostate cancer therapy in vivo. Proc Natl Acad Sci U S A. 2011 Feb 1;108(5):1850–5.

46. Heinze T, Liebert T, Heublein B, Hornig S. Functional Polymers Based on Dextran. In: Polysaccharides II. Springer Berlin Heidelberg; 2006. p. 199–291.

47. Kauffman KJ, Do C, Sharma S, Gallovic MD, Bachelder EM, Ainslie KM. Synthesis and Characterization of Acetalated Dextran Polymer and Microparticles with Ethanol as a Degradation Product. ACS Appl Mater Interfaces. 2012 Aug 22;4(8):4149–55.

48. Paine AJ, Dayan AD. Defining a tolerable concentration of methanol in alcoholic drinks. Hum Exp Toxicol. 2001 Nov 2;20(11):563–8.

49. Bachelder EM, Pino EN, Ainslie KM. Acetalated Dextran: A Tunable and Acid-Labile Biopolymer with Facile Synthesis and a Range of Applications. Chem Rev. 2017 Feb 8;117(3):1915–26.

50. Broaders KE, Cohen JA, Beaudette TT, Bachelder EM, Frechet JMJ. Acetalated dextran is a chemically and biologically tunable material for particulate immunotherapy. Proc Natl Acad Sci. 2009 Apr 7;106(14):5497–502.

51. Helaly FM, Hashem MS. Preparation and Characterization of Poly(β-Amino Ester) Capsules for Slow Release of Bioactive Material. J Encapsulation Adsorpt Sci. 2013 Sep 24;3(3):65–70.

52. Liu D, Zhang H, Mäkilä E, Fan J, Herranz-Blanco B, Wang C-F, et al. Microfluidic assisted one-step fabrication of porous silicon@acetalated dextran nanocomposites for precisely controlled combination chemotherapy. Biomaterials. 2015 Jan;39:249–59.

53. Fontana F, Shahbazi M-A, Liu D, Zhang H, Mäkilä E, Salonen J, et al. Nanovaccines: Multistaged Nanovaccines Based on Porous Silicon@Acetalated Dextran@Cancer Cell Membrane for Cancer Immunotherapy (Adv. Mater. 7/2017). Adv Mater. 2017 Feb 1;29(7).

54. Zhang H, Liu D, Wang L, Liu Z, Wu R, Janoniene A, et al. Microfluidic Encapsulation of Prickly Zinc-Doped Copper Oxide Nanoparticles with VD1142 Modified Spermine Acetalated Dextran for Efficient Cancer Therapy. Adv Healthc Mater. 2017 Jun;6(11):1601406.

55. Bauleth-Ramos T, Shahbazi M-A, Liu D, Fontana F, Correia A, Figueiredo P, et al. Nutlin-3a and Cytokine Co-loaded Spermine-Modified Acetalated Dextran Nanoparticles for Cancer Chemo-Immunotherapy. Adv Funct Mater. 2017 Sep 4;1703303.

56. Cohen JA, Beaudette TT, Cohen JL, Broaders KE, Bachelder EM, Fréchet JMJ. Acetal-Modified Dextran Microparticles with Controlled Degradation Kinetics and Surface Functionality for Gene Delivery in Phagocytic and Non-Phagocytic Cells. Adv Mater. 2010 Aug 24;22(32):3593–7.

57. Cui L, Cohen JA, Broaders KE, Beaudette TT, Fréchet JMJ. Mannosylated Dextran Nanoparticles: A pH-Sensitive System Engineered for Immunomodulation through Mannose Targeting. Bioconjug Chem. 2011 May 18;22(5):949–57.

58. Suarez SL, Muñoz A, Mitchell AC, Braden RL, Luo C, Cochran JR, et al. Degradable Acetalated Dextran Microparticles for Tunable Release of an Engineered Hepatocyte Growth Factor Fragment. ACS Biomater Sci Eng. 2016 Feb 8;2(2):197–204.

59. Delong RK, Reynolds CM, Malcolm Y, Schaeffer A, Severs T, Wanekaya A. Functionalized gold nanoparticles for the binding, stabilization, and delivery of therapeutic DNA, RNA, and other biological macromolecules. Nanotechnol Sci Appl. 2010 Sep 20;3:53–63.

60. Akerman ME, Chan WCW, Laakkonen P, Bhatia SN, Ruoslahti E. Nanocrystal targeting in vivo. Proc Natl Acad Sci U S A. 2002 Oct 1;99(20):12617–21.

61. Daou TJ, Li L, Reiss P, Josserand V, Texier I. Effect of Poly(ethylene glycol) Length on the in Vivo Behavior of Coated Quantum Dots. Langmuir. 2009 Mar 3;25(5):3040–4.

62. Boeneman K, Deschamps JR, Buckhout-White S, Prasuhn DE, Blanco-Canosa JB, Dawson PE, et al. Quantum Dot DNA Bioconjugates: Attachment Chemistry Strongly Influences the Resulting Composite Architecture. ACS Nano. 2010 Dec 28;4(12):7253–66.

63. Maldiney T, Richard C, Seguin J, Wattier N, Bessodes M, Scherman D. Effect of Core Diameter, Surface Coating, and PEG Chain Length on the Biodistribution of Persistent Luminescence Nanoparticles in Mice. ACS Nano. 2011 Feb 22;5(2):854–62.

64. Jokerst J V, Lobovkina T, Zare RN, Gambhir SS. Nanoparticle PEGylation for imaging and therapy. Nanomedicine (Lond). 2011 Jun;6(4):715–28.

65. van Vlerken LE, Vyas TK, Amiji MM. Poly(ethylene glycol)-modified Nanocarriers for Tumor-targeted and Intracellular Delivery. Pharm Res. 2007 Aug 29;24(8):1405–14.

66. Bertrand N, Leroux J-C. The journey of a drug-carrier in the body: An anatomo-physiological perspective. J Control Release. 2012 Jul 20;161(2):152–63.

67. Kanaras AG, Kamounah FS, Schaumburg K, Kiely CJ, Brust M. Thioalkylated tetraethylene glycol: a new ligand for water soluble monolayer protected gold clusters. Chem Commun (Camb). 2002 Oct 21;(20):2294–5.

68. Kwon GS. Polymeric micelles for delivery of poorly water-soluble compounds. Crit Rev Ther Drug Carrier Syst. 2003;20(5):357–403.

69. Sun Z, Tong G, Kim TH, Ma N, Niu G, Cao F, et al. PEGylated Exendin-4, a Modified GLP-1 Analog Exhibits More Potent Cardioprotection than Its Unmodified Parent Molecule on a Dose to Dose Basis in a Murine Model of Myocardial Infarction. Theranostics. 2015;5(3):240–50.

70. Zhang S, Wang J, Pan J. Baicalin-loaded PEGylated lipid nanoparticles: characterization, pharmacokinetics, and protective effects on acute myocardial ischemia in rats. Drug Deliv. 2016 Nov 21;23(9):3696–703.

71. Shao M, Yang W, Han G. Protective effects on myocardial infarction model: delivery of schisandrin B using matrix metalloproteinase-sensitive peptide-modified, PEGylated lipid nanoparticles. Int J Nanomedicine. 2017 Sep;Volume 12:7121–30.

72. Xia N, Xing Y, Wang G, Feng Q, Chen Q, Feng H, et al. Probing of EDC/NHSS-Mediated Covalent Coupling Reaction by the Immobilization of Electrochemically Active Biomolecules. Int J Electrochem Sci. 2013;8:2459–67.

73. Sperling RA, Parak WJ. Surface modification, functionalization and bioconjugation of colloidal inorganic nanoparticles. Philos Trans A Math Phys Eng Sci. 2010 Mar 28;368(1915):1333–83.

74. Grabarek Z, Gergely J. Zero-length crosslinking procedure with the use of active esters. Anal Biochem. 1990 Feb 15;185(1):131–5.

75. Jang L-S, Keng H-K. Modified fabrication process of protein chips using a short-chain self-assembled monolayer. Biomed Microdevices. 2008 Apr 12;10(2):203–11.

76. Sam S, Touahir L, Salvador Andresa J, Allongue P, Chazalviel J-N, Gouget-Laemmel AC, et al. Semiquantitative Study of the EDC/NHS Activation of Acid Terminal Groups at Modified Porous Silicon Surfaces. Langmuir. 2010 Jan 19;26(2):809–14.

77. Wang C, Yan Q, Liu H-B, Zhou X-H, Xiao S-J. Different EDC/NHS Activation Mechanisms between PAA and PMAA Brushes and the Following Amidation Reactions. Langmuir. 2011 Oct 4;27(19):12058–68.

78. Zhou Y, Andersson O, Lindberg P, Liedberg B. Reversible Hydrophobic Barriers Introduced by Microcontact Printing: Application to Protein Microarrays. Microchim Acta. 2004 Jun 1;146(3–4):193–205.

79. Wu R, Nguyen T, Marquart G, Miesen T, Mau T, Mackiewicz M. A Facile Route to Tailoring Peptide-Stabilized Gold Nanoparticles Using Glutathione as a Synthon. Molecules. 2014 May 23;19(5):6754–75.

80. Fu Y, Kao WJ. Drug release kinetics and transport mechanisms of non-degradable and degradable polymeric delivery systems. Expert Opin Drug Deliv. 2010 Apr 23;7(4):429–44.

81. Singh R, Lillard JW. Nanoparticle-based targeted drug delivery. Exp Mol Pathol. 2009 Jun;86(3):215–23.

82. Mello VA de, Ricci-Júnior E. Encapsulation of naproxen in nanostructured system: structural characterization and in vitro release studies. Quim Nova. 2011;34(6):933–9.

83. Costa P, Sousa Lobo JM. Modeling and comparison of dissolution profiles. Eur J Pharm Sci. 2001 May;13(2):123–33.

84. Ramteke KH, Dighe PA, Kharat AR, Patil S V. Review Article Mathematical Models of Drug Dissolution : A Review. Sch Acad J Pharm. 2014;3(5):388–96.

85. Lokhandwala H, Lokhandwala H, Deshpande A. KINETIC MODELING AND DISSOLUTION PROFILES COMPARISON: AN OVERVIEW. 2013;

86. Dash S, Murthy PN, Nath L, Chowdhury P. Kinetic modeling on drug release from controlled drug delivery systems. Acta Pol Pharm. 2010;67(3):217–23.

87. Rosu MC, Bratu I. Promising psyllium-based composite containing TiO2 nanoparticles as aspirin-carrier matrix. Prog Nat Sci Mater Int. 2014 Jun 1;24(3):205–9.

88. Singh NA, Mandal AKA, Khan ZA. Fabrication of PLA-PEG Nanoparticles as Delivery Systems for Improved Stability and Controlled Release of Catechin. J Nanomater. 2017 Sep 14;2017:1–9.

89. Bohrey S, Chourasiya V, Pandey A. Polymeric nanoparticles containing diazepam: preparation, optimization, characterization, in-vitro drug release and release kinetic study. Nano Converg. 2016 Dec 1;3(1):3.

90. Yang L, Fassihi R. Zero-Order Release Kinetics from a Self-Correcting Floatable Asymmetric Configuration Drug Delivery System. J Pharm Sci. 1996 Feb 1;85(2):170–3.

91. Freitas MN, Marchetti JM. Nimesulide PLA microspheres as a potential sustained release system for the treatment of inflammatory diseases. Int J Pharm. 2005 May 13;295(1–2):201–11.

92. Bravo SA, Lamas MC, Salomón CJ. In-Vitro Studies of Diclofenac Sodium Controlled-release from Biopolymeric Hydrophilic Matrices. J Pharm Pharm Sci. 2002;5(3):213–9.

93. Grassi M, Grassi G. Mathematical modelling and controlled drug delivery: matrix systems. Curr Drug Deliv. 2005 Jan;2(1):97–116.

94. Shoaib MH, Tazeen J, Merchant HA, Yousuf RI. Evaluation of drug release kinetics from ibuprofen matrix tablets using HPMC. Pak J Pharm Sci. 2006 Apr;19(2):119–24.

95. Chen S, Zhu J, Cheng J. Preparation and in vitro evaluation of a novel combined multiparticulate delayed-onset sustained-release formulation of diltiazem hydrochloride. Pharmazie. 2007 Dec;62(12):907–13.

96. Kakar S, Singh R, Semwal A. Drug release characteristics of dosage forms: a review. J Coast Life Med. 2014;2(4):332–6.

97. Välimäki MJ, Tölli MA, Kinnunen SM, Aro J, Serpi R, Pohjolainen L, et al. Discovery of Small Molecules Targeting the Synergy of Cardiac Transcription Factors GATA4 and NKX2-5. J Med Chem. 2017 Sep 28;60(18):7781–98.

98. Conde J, Dias JT, Grazú V, Moros M, Baptista P V, de la Fuente JM. Revisiting 30 years of biofunctionalization and surface chemistry of inorganic nanoparticles for nanomedicine. Front Chem. 2014;2:48.

99. Kuznetsov A V, Javadov S, Sickinger S, Frotschnig S, Grimm M. H9c2 and HL-1 cells demonstrate distinct features of energy metabolism, mitochondrial function and sensitivity to hypoxia-reoxygenation. Biochim Biophys Acta. 2015 Feb;1853(2):276–84.

100. Abas L, Bogoyevitch MA, Guppy M. Mitochondrial ATP production is necessary for activation of the extracellular-signal-regulated kinases during ischaemia/reperfusion in rat myocyte-derived H9c2 cells. Biochem J. 2000 Jul 1;349(Pt 1):119–26.

101. Muscari C, Gamberini C, Bonafe' F, Giordano E, Bianchi C, Lenaz G, et al. Evaluation of cellular energetics by the pasteur effect in intact cardiomyoblasts and isolated perfused hearts. Mol Cell Biochem. 2004 Mar;258(1–2):91–7.

102. Herrmann J, Bodmeier R. Biodegradable, somatostatin acetate containing microspheres prepared by various aqueous and non-aqueous solvent evaporation methods. Eur J Pharm Biopharm. 1998 Jan;45(1):75–82.

103. Jeffery H, Davis SS, O'Hagan DT. The preparation and characterization of poly(lactide-co-glycolide) microparticles. II. The entrapment of a model protein using a (water-in-oil)-in-water emulsion solvent evaporation technique. Pharm Res. 1993 Mar;10(3):362–8.

104. Sansdrap P, Moës AJ. Influence of manufacturing parameters on the size characteristics and the release profiles of nifedipine from poly(DL-lactide-co-glycolide) microspheres. Int J Pharm. 1993 Aug 31;98(1–3):157–64.

105. Carrio A, Schwach G, Coudane J, Vert M. Preparation and degradation of surfactant-free PLAGA microspheres. J Control Release. 1995 Nov;37(1–2):113–21.

106. Yang Y. Morphology, drug distribution, and in vitro release profiles of biodegradable polymeric microspheres containing protein fabricated by double-emulsion solvent extraction/evaporation method. Biomaterials. 2001 Feb;22(3):231–41.

107. Budhian A, Siegel SJ, Winey KI. Haloperidol-loaded PLGA nanoparticles: Systematic study of particle size and drug content. Int J Pharm. 2007 May 24;336(2):367–75.

108. Gorner T. Lidocaine-loaded biodegradable nanospheres. I. Optimization of the drug incorporation into the polymer matrix. J Control Release. 1999 Feb 22;57(3):259–68.

109. Budhian A, Siegel SJ, Winey KI. Production of haloperidol-loaded PLGA nanoparticles for extended controlled drug release of haloperidol. J Microencapsul. 2005 Jan 8;22(7):773–85.

110. Krishnamachari Y, Madan P, Lin S. Development of pH- and time-dependent oral microparticles to optimize budesonide delivery to ileum and colon. Int J Pharm. 2007 Jun 29;338(1–2):238–47.

111. André-Abrant A, Taverdet J-L, Jay J. Microencapsulation par évaporation de solvant. Eur Polym J. 2001 May;37(5):955–63.

112. Vashist SK. Comparison of 1-Ethyl-3-(3-Dimethylaminopropyl) Carbodiimide Based Strategies to Crosslink Antibodies on Amine-Functionalized Platforms for Immunodiagnostic Applications. Diagnostics. 2012 Aug 27;2(4):23–33.

113. Puertas S, Batalla P, Moros M, Polo E, del Pino P, Guisán JM, et al. Taking Advantage of Unspecific Interactions to Produce Highly Active Magnetic Nanoparticle−Antibody Conjugates. ACS Nano. 2011 Jun 28;5(6):4521–8.

114. Bergeron RJ, Weimar WR, Wu Q, Feng Y, McManis JS. Polyamine analogue regulation of NMDA MK-801 binding: A structure-activity study. J Med Chem. 1996 Jan 20;39(26):5257–66.

115. Jazayeri MH, Amani H, Pourfatollah AA, Pazoki-Toroudi H, Sedighimoghaddam B. Various methods of gold nanoparticles (GNPs) conjugation to antibodies. Sens Bio-Sensing Res. 2016 Jul;9:17–22.

116. Fuentes M, Mateo C, Guisán JM, Fernández-Lafuente R. Preparation of inert magnetic nano-particles for the directed immobilization of antibodies. Biosens Bioelectron. 2005 Jan;20(7):1380–7.

117. Lu J, Jackson JK, Gleave ME, Burt HM. The preparation and characterization of anti-VEGFR2 conjugated, paclitaxel-loaded PLLA or PLGA microspheres for the systemic targeting of human prostate tumors. Cancer Chemother Pharmacol. 2008 May 15;61(6):997–1005.

118. Huang X, Jain PK, El-Sayed IH, El-Sayed MA. Plasmonic photothermal therapy (PPTT) using gold nanoparticles. Lasers Med Sci. 2008 Jul 3;23(3):217–28.

119. Albanese A, Chan WCW. Effect of Gold Nanoparticle Aggregation on Cell Uptake and Toxicity. ACS Nano. 2011 Jul 26;5(7):5478–89.

120. Limbach LK, Li Y, Grass RN, Brunner TJ, Hintermann MA, Muller M, et al. Oxide nanoparticle uptake in human lung fibroblasts: effects of particle size, agglomeration, and diffusion at low concentrations. Environ Sci Technol. 2005 Dec 1;39(23):9370–6.

121. Wick P, Manser P, Limbach L, Dettlaffweglikowska U, Krumeich F, Roth S, et al. The degree and kind of agglomeration affect carbon nanotube cytotoxicity. Toxicol Lett. 2007 Jan 30;168(2):121–31.

122. Knop K, Hoogenboom R, Fischer D, Schubert US. Poly(ethylene glycol) in Drug Delivery: Pros and Cons as Well as Potential Alternatives. Angew Chemie Int Ed. 2010 Aug 23;49(36):6288–308.

123. Magenheim B, Levy MY, Benita S. A new in vitro technique for the evaluation of drug release profile from colloidal carriers - ultrafiltration technique at low pressure. Int J Pharm. 1993 Jun;94(1–3):115–23.

124. Fresta M, Puglisi G, Giammona G, Cavallaro G, Micali N, Furneri PM. Pefloxacine mesilate- and ofloxacin-loaded polyethylcyanoacrylate nanoparticles: characterization of the colloidal drug carrier formulation. J Pharm Sci. 1995 Jul;84(7):895–902.

125. Gómez-Gaete C, Tsapis N, Besnard M, Bochot A, Fattal E. Encapsulation of dexamethasone into biodegradable polymeric nanoparticles. Int J Pharm. 2007 Mar 1;331(2):153–9.

126. Davaran S, Rashidi MR, Pourabbas B, Dadashzadeh M, Haghshenas NM. Adriamycin release from poly(lactide-coglycolide)-polyethylene glycol nanoparticles: synthesis, and in vitro characterization. Int J Nanomedicine. 2006;1(4):535–9.

127. Jeong YI, Nah JW, Lee HC, Kim SH, Cho CS. Adriamycin release from flower-type polymeric micelle based on star-block copolymer composed of poly(gamma-benzyl L-glutamate) as the hydrophobic part and poly(ethylene oxide) as the hydrophilic part. Int J Pharm. 1999 Oct 15;188(1):49–58.

128. Freitas S, Merkle HP, Gander B. Microencapsulation by solvent extraction/evaporation: reviewing the state of the art of microsphere preparation process technology. J Control Release. 2005 Feb 2;102(2):313–32.

129. Moore TL, Rodriguez-Lorenzo L, Hirsch V, Balog S, Urban D, Jud C, et al. Nanoparticle colloidal stability in cell culture media and impact on cellular interactions. Chem Soc Rev. 2015 Oct 7;44(17):6287–305.

130. Jiang X, Weise S, Hafner M, Rocker C, Zhang F, Parak WJ, et al. Quantitative analysis of the protein corona on FePt nanoparticles formed by transferrin binding. J R Soc Interface. 2010 Feb 6;7(Suppl_1):S5–13.

131. Cho EC, Zhang Q, Xia Y. The effect of sedimentation and diffusion on cellular uptake of gold nanoparticles. Nat Nanotechnol. 2011 Jun 24;6(6):385–91.

132. Chern CS, Lee CK, Ho CC. Electrostatic interaction between chitosan-modified latex particles and bovine serum albumin. Colloid Polym Sci. 1999 Oct 1;277(10):979–85.

133. Karmali PP, Simberg D. Interactions of nanoparticles with plasma proteins: implication on clearance and toxicity of drug delivery systems. Expert Opin Drug Deliv. 2011 Mar 4;8(3):343–57.

134. Baalousha M. Aggregation and disaggregation of iron oxide nanoparticles: Influence of particle concentration, pH and natural organic matter. Sci Total Environ. 2009 Mar 1;407(6):2093–101.

135. Cedervall T, Lynch I, Lindman S, Berggard T, Thulin E, Nilsson H, et al. Understanding the nanoparticle-protein corona using methods to quantify exchange rates and affinities of proteins for nanoparticles. Proc Natl Acad Sci. 2007 Feb 13;104(7):2050–5.

136. Lesniak A, Fenaroli F, Monopoli MP, Åberg C, Dawson KA, Salvati A. Effects of the Presence or Absence of a Protein Corona on Silica Nanoparticle Uptake and Impact on Cells. ACS Nano. 2012 Jul 24;6(7):5845–57.

137. Larson TA, Joshi PP, Sokolov K. Preventing protein adsorption and macrophage uptake of gold nanoparticles via a hydrophobic shield. ACS Nano. 2012 Oct 23;6(10):9182–90.

138. Dobrovolskaia MA, Patri AK, Zheng J, Clogston JD, Ayub N, Aggarwal P, et al. Interaction of colloidal gold nanoparticles with human blood: effects on particle size and analysis of plasma protein binding profiles. Nanomedicine Nanotechnology, Biol Med. 2009 Jun;5(2):106–17.

139. Avgoustakis K, Beletsi A, Panagi Z, Klepetsanis P, Livaniou E, Evangelatos G, et al. Effect of copolymer composition on the physicochemical characteristics, in vitro stability, and biodistribution of PLGA-mPEG nanoparticles. Int J Pharm. 2003 Jun 18;259(1–2):115–27.

140. Louguet S, Kumar AC, Guidolin N, Sigaud G, Duguet E, Lecommandoux S, et al. Control of the PEO Chain Conformation on Nanoparticles by Adsorption of PEO- *block* -Poly(l -lysine) Copolymers and Its Significance on Colloidal Stability and Protein Repellency. Langmuir. 2011 Nov 1;27(21):12891–901.

141. Fröhlich E. The role of surface charge in cellular uptake and cytotoxicity of medical nanoparticles. Int J Nanomedicine. 2012 Nov;7:5577.

142. Näkki S, Rytkönen J, Nissinen T, Florea C, Riikonen J, Ek P, et al. Improved stability and biocompatibility of nanostructured silicon drug carrier for intravenous administration. Acta Biomater. 2015 Feb 1;13:207–15.

143. Luo X, Feng M, Pan S, Wen Y, Zhang W, Wu C. Charge shielding effects on gene delivery of polyethylenimine/DNA complexes: PEGylation and phospholipid coating. J Mater Sci Mater Med. 2012 Jul 6;23(7):1685–95.

144. Ferreira MPA, Ranjan S, Kinnunen S, Correia A, Talman V, Mäkilä E, et al. Drug-Loaded Multifunctional Nanoparticles Targeted to the Endocardial Layer of the Injured Heart Modulate Hypertrophic Signaling. Small. 2017 Sep;13(33):1701276.

145. Ferreira MPA, Ranjan S, Correia AMR, Mäkilä EM, Kinnunen SM, Zhang H, et al. In vitro and in vivo assessment of heart-homing porous silicon nanoparticles. Biomaterials. 2016 Jul;94:93–104.